

# FOURTH-ORDER UNIFORMLY ACCURATE INTEGRATORS WITH LONG TIME NEAR CONSERVATIONS FOR THE NONLINEAR DIRAC EQUATION IN THE NONRELATIVISTIC REGIME \*

LINA WANG<sup>†</sup>, BIN WANG<sup>‡</sup>, AND JIYONG LI<sup>§</sup>

**Abstract.** In this paper, we propose two novel fourth-order integrators that exhibit uniformly high accuracy and long-term near conservations for solving the nonlinear Dirac equation (NLDE) in the nonrelativistic regime. In this regime, the solution of the NLDE exhibits highly oscillatory behavior in time, characterized by a wavelength of  $\mathcal{O}(\varepsilon^2)$  with a small parameter  $\varepsilon > 0$ . To ensure uniform temporal accuracy, we employ a two-scale approach in conjunction with exponential integrators, utilizing operator decomposition techniques for the NLDE. The proposed methods are rigorously proved to achieve fourth-order uniform accuracy in time for all  $\varepsilon \in (0, 1]$ . Furthermore, we successfully incorporate symmetry into the integrator, and the long-term near conservation properties are analyzed through the modulated Fourier expansion. The proposed schemes are readily extendable to linear Dirac equations incorporating magnetic potentials, the dynamics of traveling wave solutions and the two/three-dimensional Dirac equations. The validity of all theoretical findings and extensions is numerically substantiated through a series of numerical experiments.

**Key words.** Nonlinear Dirac equation, Nonrelativistic regime, Uniformly accurate integrators, Long time near conservation, Two-scale formulation

**AMS subject classifications.** 35Q41, 65M70, 65N35, 81Q05

**1. Introduction.** The Dirac equation, first proposed by Paul Dirac in 1928, serves as a fundamental framework for describing all massive spin-1/2 particles, including electrons, positrons, and so on [25]. As a cornerstone of quantum physics, this equation elegantly unifies the principles of quantum mechanics and special relativity. In recent years, the Dirac equation has gained renewed significance due to its applicability in diverse theoretical studies, such as the electronic properties of graphite and graphene [50, 19, 48], interactions of molecules with intense laser fields [29, 30], and Bose-Einstein condensation phenomena [6, 34]. Consequently, the numerical solution of the Dirac equation has garnered substantial attention from researchers across various disciplines.

In the study of the Dirac equation, the choice of parameters gives rise to a variety of regimes, among which are the classical regime, the massless regime, the semi-classical regime [21, 56], and the non-relativistic regime ([4, 5, 57]). In this work, we focus on the nonlinear Dirac equation (NLDE) in the nonrelativistic regime, specifically in the absence of a magnetic potential [2]. As demonstrated in [3, 11], the three-dimensional Dirac equation, expressed in its four-component form to describe the time evolution of spin-1/2 massive particles, can be reduced to a two-component form in two dimensions and one dimension under appropriate assumptions on the electromagnetic potentials. Therefore, here we focus on the two-component form and it is noted that all the integrators developed in this paper can be straightforwardly extended to the Dirac equation of a four-component form. In one or two spatial dimensions, the equation can be expressed in a two-component form, characterized by a complex-valued vector wave function  $\Phi := \Phi(t, \mathbf{x}) = (\phi_1(t, \mathbf{x}), \phi_2(t, \mathbf{x}))^\top \in \mathbb{C}^2$ :

(1.1)

$$i\partial_t \Phi = \left( -\frac{i}{\varepsilon} \sum_{j=1}^d \sigma_j \partial_j + \frac{\sigma_3}{\varepsilon^2} \right) \Phi + V(\mathbf{x})\Phi + \mathbf{F}(\Phi)\Phi, \quad d = 1, 2, \quad t > 0, \quad \Phi(0, \mathbf{x}) = \Phi_0(\mathbf{x}), \quad \mathbf{x} \in \mathbb{R}^d,$$

where  $i = \sqrt{-1}$  is the imaginary unit,  $t$  is time,  $\varepsilon \in (0, 1]$  is a dimensionless parameter inversely proportional to the speed of light,  $\mathbf{x} = (x_1, \dots, x_d)^\top \in \mathbb{R}^d$  is the spatial coordinate vector,  $\partial_j = \frac{\partial}{\partial x_j}$  ( $j = 1, \dots, d$ ),  $V(\mathbf{x})$  is a real-valued function denoting the external electric potential, and  $\sigma_1, \sigma_2, \sigma_3$

\*Submitted to the editors DATE.

**Funding:** B. Wang is supported by NSFC 12371403.

<sup>†</sup>School of Mathematics and Statistics, Xi'an Jiaotong University, 710049 Xi'an, China (wanglina@stu.xjtu.edu.cn).

<sup>‡</sup>Corresponding author. School of Mathematics and Statistics, Xi'an Jiaotong University, 710049 Xi'an, China (wangbinmaths@xjtu.edu.cn).

<sup>§</sup>School of Mathematics Science, Hebei Key Laboratory of Computatioanal Mathematics and Applications, Hebei International Joint Research Center for Mathematics and Interdisciplinary Science, Hebei Normal University, Shijiazhuang 050024, China (lijong406@163.com).

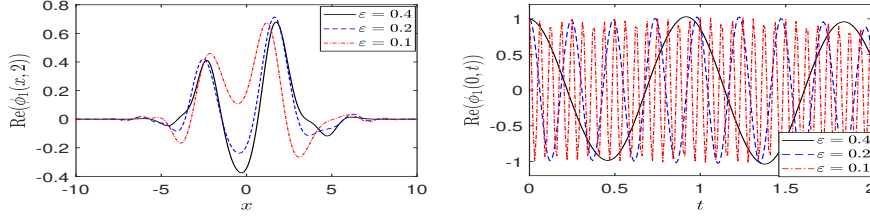


FIG. 1. The solution  $\phi_1(t=2, x)$  and  $\phi_1(t, x=0)$  of the Dirac equation (1.1) with  $d=1$  for different  $\varepsilon$  ( $\text{Re}(\phi_1)$  denotes the real part of  $\phi_1$ ).

are the Pauli matrices defined as

$$(1.2) \quad \sigma_1 = \begin{pmatrix} 0 & 1 \\ 1 & 0 \end{pmatrix}, \quad \sigma_2 = \begin{pmatrix} 0 & -i \\ i & 0 \end{pmatrix}, \quad \sigma_3 = \begin{pmatrix} 1 & 0 \\ 0 & -1 \end{pmatrix}.$$

The commonly used form for nonlinearity  $\mathbf{F}(\Phi)$  in (1.1) is

$$(1.3) \quad \mathbf{F}(\Phi) = \lambda_1(\Phi^* \sigma_3 \Phi) \sigma_3 + \lambda_2 |\Phi|^2 I_2,$$

with  $|\Phi|^2 = \Phi^* \Phi$ , where  $\lambda_1, \lambda_2 \in \mathbb{R}$  are two given real constants,  $\Phi^* = \overline{\Phi}^\top$  is the complex conjugate transpose of  $\Phi$ . The nonlinearity is inspired by two distinct physical contexts: the Soler model in quantum field theory, where  $\lambda_1 \neq 0$  and  $\lambda_2 = 0$  [31, 33], and the Bose-Einstein condensation (BEC) with chiral confinement and spin-orbit coupling, where  $\lambda_1 = 0$  and  $\lambda_2 \neq 0$  [22, 34, 35]. It is well known that the solution of NLDE (1.1) conserves the total mass

$$(1.4) \quad M(\Phi) := \int_{\mathbb{R}^d} |\Phi(t, \mathbf{x})|^2 d\mathbf{x} = \int_{\mathbb{R}^d} \sum_{j=1}^2 |\phi_j(t, \mathbf{x})|^2 d\mathbf{x} \equiv M(\Phi_0),$$

and the total energy

$$(1.5) \quad E(\Phi) := \int_{\mathbb{R}^d} \left( -\frac{i}{\varepsilon} \sum_{j=1}^d \Phi^* \sigma_j \partial_j \Phi + \frac{1}{\varepsilon^2} \Phi^* \sigma_3 \Phi + V(\mathbf{x}) |\Phi|^2 + \frac{\lambda_1}{2} (\Phi^* \sigma_3 \Phi)^2 + \frac{\lambda_2}{2} |\Phi|^4 \right) d\mathbf{x} \equiv E(\Phi_0).$$

From an analytical perspective, the existence and diversity of bound states or standing wave solutions have been extensively studied in [1, 14, 20, 26, 27]. Notably, for the specific choice of  $F(\Phi)$  with  $\lambda_1 = -1$ ,  $\lambda_2 = 0$  and  $d=1$ ,  $V(x) = 0$ , exact soliton solutions to the Dirac equation (1.1) have been established [47, 53, 51, 57]. On the numerical front, a variety of methods have been developed to solve the Dirac equation (1.1) such as finite difference time domain (FDTD) methods [3, 15, 38, 49], time-splitting and time-splitting Fourier pseudospectral (TSFP) methods [2, 3, 11, 13, 32, 42], exponential wave integrator Fourier pseudospectral (EWI-FP) methods [3, 44], and Runge-Kutta discontinuous Galerkin methods [41]. It is worth noting that when  $0 < \varepsilon \ll 1$ , the solution of the Dirac equation (1.1) exhibits wave propagation with spatial wavelengths of  $\mathcal{O}(1)$  and temporal wavelengths of  $\mathcal{O}(\varepsilon^2)$ . To further illustrate this behavior, Figure 1 presents the numerical solution of the Dirac equation (1.1) with  $d=1$ ,  $V(x) = \frac{1-x}{1+x^2}$ ,  $\lambda_1 = -1$ ,  $\lambda_2 = 0$  and  $\Phi_0(x) = (\exp(-x^2/2), \exp(-(x-1)^2/2))^\top$  for different  $\varepsilon$ . It can be clearly observed that the small temporal wavelength of the solution induces high temporal oscillations, posing significant challenges for both theoretical analysis and classical numerical discretization in the nonrelativistic regime where  $0 < \varepsilon \ll 1$ . To ensure the accuracy of numerical solutions, the time step and spatial mesh size in traditional methods have to depend on  $\varepsilon$ . Consequently, developing numerical methods that permit the use of  $\varepsilon$ -independent time step is both essential and highly challenging to effectively address these temporal oscillations.

Recently, significant advancements have been achieved in the numerical solution of highly oscillatory problems through the development of uniformly accurate (UA) schemes [7, 8, 12, 23, 24]. Both

the time stepsize and the accuracy are independent of  $\varepsilon$ , which is the primary advantage of UA methods. Improved error bounds on splitting methods for the Dirac equation with weakly nonlinear or small potentials have been analyzed in [9, 10]. Utilizing two-scale formulation, two numerical schemes with first- and second-order uniform accuracies are constructed for the nonlinear Dirac equation in the nonrelativistic regime [43]. The work [4] proposed a novel method which achieves first-order uniform accuracy for all  $\varepsilon \in (0, 1]$  and optimal second-order accuracy in the regimes when either  $\varepsilon = O(1)$  or  $0 < \varepsilon \lesssim \Delta t$  for a time stepsize  $\Delta t$ . Another method with similar accuracy has been proposed in [18] also for the nonlinear Dirac equation. Additionally, uniform first- and second-order Picard iteration approaches have been applied to the nonlinear Dirac equation in [17], and UA methods up to third order have been formulated for the linear Dirac equation in [16]. Despite these great advancements, the existing UA methods are limited to second-order temporal accuracy for the nonlinear Dirac equation and third-order temporal accuracy for the linear case, and their formulation and analysis are computationally intensive. Moreover, while various structure-preserving methods have been investigated for the mass and energy conservation properties of the Dirac equation [44, 45], a thorough long-time analysis of UA schemes for the nonlinear Dirac equation is notably absent. In summary, for the nonlinear Dirac equation (1.1) in the nonrelativistic limit, it seems that all the UA schemes are constrained to second-order accuracy, and a detailed long-time analysis of their conservation properties is absent.

The objective of this work is to develop and analyze a family of high order uniformly accurate integrators and the main contributions are as follows. a) This paper provides a general framework for the construction of high order UA algorithms for the NLDE. Compared with the existing UA methods, the accuracy of the proposed integrators are improved to fourth order, which is very competitive in the numerical computation of the NLDE. b) Utilizing the robust modulated Fourier expansion technique, we conduct a long-time analysis of the developed symmetric UA algorithm. The analysis reveals that the novel method maintains the energy and mass conservations of the NLDE over long times.

The article is structured as follows. In Section 2, we present the formulation of novel schemes. Section 3 studies the fourth-order uniform error bounds and long-time near conservations of the proposed methods. In Section 4, five numerical experiments are conducted for various one-dimensional and two-dimensional Dirac equations, numerically demonstrating the accuracy and long-time behaviour. The last section is devoted to the conclusions of this paper.

**2. Formulation of the method.** Without loss of generality, we restrict this section to the one-dimensional case ( $d = 1$ ) of (1.1). The extension to the two-dimensional case, as well as to the four-component form in three dimensions for tensor grids, is straightforward.

**2.1. Transformation of the equation.** For integer  $m > 0$ ,  $\Omega = [a, b]$ , we denote by  $H^m(\Omega)$  the standard Sobolev space. Introduce the Dirac operator [2]

$$(2.1) \quad Q^\varepsilon = -i\varepsilon\sigma_1\partial_x + \sigma_3, \quad x \in \mathbb{R}.$$

In the phase space (Fourier domain),  $Q^\varepsilon$  is diagonalizable and can be decomposed as

$$(2.2) \quad Q^\varepsilon = \sqrt{Id - \varepsilon^2\Delta}\Pi_+^\varepsilon - \sqrt{Id - \varepsilon^2\Delta}\Pi_-^\varepsilon,$$

where  $\Delta = \partial_{xx}$  represents the one-dimensional Laplace operator,  $Id$  denotes the identity operator, and  $\Pi_\pm^\varepsilon : (H^m(\mathbb{R}))^2 \rightarrow (H^m(\mathbb{R}))^2$  are projector operators

$$(2.3) \quad \Pi_+^\varepsilon = \frac{1}{2}[Id + (Id - \varepsilon^2\Delta)^{-1/2}Q^\varepsilon], \quad \Pi_-^\varepsilon = \frac{1}{2}[Id - (Id - \varepsilon^2\Delta)^{-1/2}Q^\varepsilon].$$

It can be verified that the projection operators  $\Pi_+^\varepsilon$  and  $\Pi_-^\varepsilon$  satisfy  $\Pi_+^\varepsilon + \Pi_-^\varepsilon = Id$ ,  $\Pi_+^\varepsilon\Pi_-^\varepsilon = \Pi_-^\varepsilon\Pi_+^\varepsilon = 0$  and  $(\Pi_\pm^\varepsilon)^2 = \Pi_\pm^\varepsilon$ . Furthermore, through Taylor expansion, we obtain

$$(2.4) \quad \Pi_\pm^\varepsilon = \Pi_\pm^0 \pm \varepsilon\mathcal{R}_1 = \Pi_\pm^0 \mp i\frac{\varepsilon}{2}\sigma_1\partial_x \pm \varepsilon^2\mathcal{R}_2, \quad \Pi_+^0 = \text{diag}(1, 0), \quad \Pi_-^0 = \text{diag}(0, 1),$$

with  $\mathcal{R}_1 : (H^m(\mathbb{R}))^2 \rightarrow (H^{m-1}(\mathbb{R}))^2$  for  $m \geq 1$  and  $\mathcal{R}_2 : (H^m(\mathbb{R}))^2 \rightarrow (H^{m-2}(\mathbb{R}))^2$  for  $m \geq 2$  which are uniformly bounded w.r.t  $\varepsilon$ . Denote

$$(2.5) \quad \mathcal{D}^\varepsilon = \frac{1}{\varepsilon^2}(\sqrt{Id - \varepsilon^2\Delta} - Id) = -(\sqrt{Id - \varepsilon^2\Delta} + Id)^{-1}\Delta.$$

This is an uniformly bounded mapping from  $(H^m(\mathbb{R}))^2 \rightarrow (H^{m-2}(\mathbb{R}))^2$  for  $m \geq 2$ . Moreover, it satisfies the inequality  $0 \leq \mathcal{D}^\varepsilon \leq -\frac{1}{2}\Delta$  for all  $\varepsilon > 0$ . Consequently, the operator  $e^{\frac{it}{\varepsilon^2}Q^\varepsilon}$  can be expressed as

$$(2.6) \quad e^{\frac{it}{\varepsilon^2}Q^\varepsilon} = e^{\frac{it}{\varepsilon^2}(\sqrt{Id-\varepsilon^2\Delta}\Pi_+^\varepsilon - \sqrt{Id-\varepsilon^2\Delta}\Pi_-^\varepsilon)} = e^{\frac{it}{\varepsilon^2}}e^{it\mathcal{D}^\varepsilon}\Pi_+^\varepsilon + e^{-\frac{it}{\varepsilon^2}}e^{-it\mathcal{D}^\varepsilon}\Pi_-^\varepsilon.$$

Using the operator  $Q^\varepsilon$ , the NLDE (1.1) can be rewritten as

$$(2.7) \quad \begin{aligned} \partial_t \Phi(t, x) &= \frac{-iQ^\varepsilon}{\varepsilon^2} \Phi(t, x) - i \left( V(x)\Phi(t, x) + \mathbf{F}(\Phi(t, x))\Phi(t, x) \right), \quad x \in \Omega, \\ \Phi(0, x) &= \Phi_0(x), \quad x \in \overline{\Omega}, \quad \Phi(t, a) = \Phi(t, b), \quad t \in [0, T], \end{aligned}$$

where  $\Omega = (a, b)$  is a bounded domain with periodic boundary conditions.

To filter out the dominant oscillations in (2.7), we introduce a transformed variable

$$(2.8) \quad \Psi(t, x) = (\psi_1(t, x), \psi_2(t, x)) := e^{\frac{itQ^\varepsilon}{\varepsilon^2}} \Phi(t, x), \quad x \in \Omega.$$

Then the system (2.7) is transformed into

$$(2.9) \quad \partial_t \Psi(t, x) = e^{\frac{itQ^\varepsilon}{\varepsilon^2}} g(e^{-\frac{itQ^\varepsilon}{\varepsilon^2}} \Psi(t, x)), \quad \Psi(0, x) = \Phi_0(x), \quad t \in (0, T],$$

where  $g(\Phi) = -i(V(x)\Phi(t, x) + \mathbf{F}(\Phi(t, x))\Phi(t, x))$ . By (2.6), it follows that

$$(2.10) \quad \partial_t \Psi(t, x) = (e^{\frac{it}{\varepsilon^2}}e^{it\mathcal{D}^\varepsilon}\Pi_+^\varepsilon + e^{-\frac{it}{\varepsilon^2}}e^{-it\mathcal{D}^\varepsilon}\Pi_-^\varepsilon) g((e^{-\frac{it}{\varepsilon^2}}e^{-it\mathcal{D}^\varepsilon}\Pi_+^\varepsilon + e^{\frac{it}{\varepsilon^2}}e^{it\mathcal{D}^\varepsilon}\Pi_-^\varepsilon) \Psi(t, x)),$$

where inserting (2.1) into (2.3) gives

$$\Pi_+^\varepsilon = \frac{1}{2} \begin{pmatrix} 1 + \delta & -i\varepsilon\partial_x\delta \\ -i\varepsilon\partial_x\delta & 1 - \delta \end{pmatrix}, \quad \Pi_-^\varepsilon = \frac{1}{2} \begin{pmatrix} 1 - \delta & i\varepsilon\partial_x\delta \\ i\varepsilon\partial_x\delta & 1 + \delta \end{pmatrix}$$

with  $\delta = (1 - \varepsilon^2\Delta)^{-\frac{1}{2}}$ .

**2.2. Two-scale formulation and its initial value.** It can be observed that (2.9) involves two distinct time scales, the fast scale  $t/\varepsilon^2$  and the slow scale  $t$ . For small  $\varepsilon$ , the fast scale  $\tau$  varies significantly more rapidly than the slow scale  $t$ . To address this, we derive a two-scale formulation by explicitly separating the fast scale  $t/\varepsilon^2$  from the slow scale  $t$ . Specifically, we introduce an augmented system of the Dirac equation, governed by the augmented solution  $U(t, \tau, x)$ , which is  $2\pi$  periodic in  $\tau$ . Here,  $U(t, \tau, x) = (U_1(t, \tau, x), U_2(t, \tau, x))$  coincides with the original solution  $\Psi(t, x)$  when  $\tau = t/\varepsilon^2$ , i.e.,  $\Psi(t, x) = U(t, t/\varepsilon^2, x)$ . Set

$$(2.11) \quad G(t, \tau, U) = (e^{i\tau}e^{it\mathcal{D}^\varepsilon}\Pi_+^\varepsilon + e^{-i\tau}e^{-it\mathcal{D}^\varepsilon}\Pi_-^\varepsilon) g((e^{-i\tau}e^{-it\mathcal{D}^\varepsilon}\Pi_+^\varepsilon + e^{i\tau}e^{it\mathcal{D}^\varepsilon}\Pi_-^\varepsilon) U).$$

According to (2.10), we obtain the following two-scale equation of NLDE

$$(2.12) \quad \partial_t U(t, \tau, x) + \frac{1}{\varepsilon^2} \partial_\tau U(t, \tau, x) = G(t, \tau, U(t, \tau, x)), \quad t \in [0, T], \quad x \in \Omega, \quad \tau \in \mathbb{T}_\tau,$$

where  $\mathbb{T}_\tau := \mathbb{R}/(2\pi\mathbb{Z})$  denotes the torus. It is noted that the initial value only needs to satisfy  $U(0, 0, x) = \Phi_0(x)$  and for  $U(0, \tau, x)$ , it can be designed as follows.

For a periodic function  $v(\cdot)$  on  $\mathbb{T}_\tau$ , we define the averaging, differentiation and its inversion operators as

$$\Pi v := \frac{1}{2\pi} \int_0^{2\pi} v(\tau) d\tau, \quad L := \partial_\tau, \quad L^{-1}v := (I - \Pi) \int_0^\tau v(s) ds, \quad A := L^{-1}(I - \Pi).$$

The solution  $U(t, \tau, x)$  of (2.12) is expressed through the Chapman-Enskog expansion [23, 24]

$$(2.13) \quad U(t, \tau, x) = \underline{U}(t, x) + h(t, \tau, x),$$

where  $\underline{U}(t, x) := \Pi U(t, \tau, x)$  is the averaged part and  $h(t, \tau, x)$  is the correction part which satisfies  $\Pi h(t, \tau, x) = 0$ . Acting the operator  $\Pi$  to both sides of (2.12), we derive the following result

$$(2.14) \quad \partial_t \underline{U}(t, x) = \Pi G(t, \tau, \underline{U}(t, x) + h(t, \tau, x)).$$

Subtracting the above from (2.12) leads to

$$(2.15) \quad \partial_t h(t, \tau, x) + \frac{1}{\varepsilon^2} \partial_\tau h(t, \tau, x) = (I - \Pi)G(t, \tau, \underline{U}(t, x) + h(t, \tau, x)),$$

which by inverting  $L = \partial_\tau$  can be rewritten as

$$(2.16) \quad h(t, \tau, x) = \varepsilon^2 (AG(t, \tau, \underline{U}(t, x) + h(t, \tau, x)) - L^{-1}(\partial_t h(t, \tau, x))).$$

From (2.16), it is evident that  $h = \mathcal{O}(\varepsilon^2)$  holds formally, motivating the consideration of the following asymptotic expansion:

$$(2.17) \quad h(t, \tau, x) = \varepsilon^2 h_1(t, \tau, \underline{U}(t, x)) + \varepsilon^4 h_2(t, \tau, \underline{U}(t, x)) + \varepsilon^6 h_3(t, \tau, \underline{U}(t, x)) + \mathcal{O}(\varepsilon^8),$$

with some  $h_1, h_2, h_3 = \mathcal{O}(1)$  to be determined.

Substituting (2.17) into (2.16) and expanding  $G(t, \tau, \cdot)$  as a Taylor series around  $\underline{U}$ , we have

$$(2.18) \quad \begin{aligned} \varepsilon^2 h_1 + \varepsilon^4 h_2 + \varepsilon^6 h_3 + \mathcal{O}(\varepsilon^8) &= \varepsilon^2 AG(t, \tau, \underline{U}) + \varepsilon^2 A \partial_u G(t, \tau, \underline{U})(\varepsilon^2 h_1 + \varepsilon^4 h_2) \\ &+ \frac{1}{2} \varepsilon^2 A \partial_u^2 G(t, \tau, \underline{U})(\varepsilon^2 h_1, \varepsilon^2 h_1) - \varepsilon^2 L^{-1}(\varepsilon^2 \partial_t h_1 + \varepsilon^4 \partial_t h_2) + \mathcal{O}(\varepsilon^8). \end{aligned}$$

By comparing the coefficients of  $\varepsilon^{2j}$  for  $j = 1, 2, 3$ , we derive the following relationships:

$$(2.19) \quad \begin{aligned} h_1(t, \tau, \underline{U}) &:= AG(t, \tau, \underline{U}), \\ h_2(t, \tau, \underline{U}) &:= A \partial_u G(t, \tau, \underline{U}) AG(t, \tau, \underline{U}) - A^2 \partial_t G(t, \tau, \underline{U}) - A^2 \partial_u G(t, \tau, \underline{U}) \Pi G(t, \tau, \underline{U}), \\ h_3(t, \tau, \underline{U}) &:= A \partial_u G(t, \tau, \underline{U}) h_2 + \frac{1}{2} A \partial_u^2 G(t, \tau, \underline{U})(h_1, h_1) - A^2 \partial_{ut} G(t, \tau, \underline{U}) AG(t, \tau, \underline{U}) \\ &- A^2 \partial_u^2 G(t, \tau, \underline{U})(\Pi G(t, \tau, \underline{U}), AG(t, \tau, \underline{U})) - A^2 \partial_u G(t, \tau, \underline{U}) A \partial_t G(t, \tau, \underline{U}) \\ &- A^2 \partial_u G(t, \tau, \underline{U}) A \partial_u G(t, \tau, \underline{U}) \Pi G(t, \tau, \underline{U}) \\ &- A^2 \partial_u G(t, \tau, \underline{U})(\Pi \partial_u G(t, \tau, \underline{U}), AG(t, \tau, \underline{U})) + A^3 \partial_t^2 G(t, \tau, \underline{U}) \\ &+ 2A^3 \partial_{tu} G(t, \tau, \underline{U}) \Pi G(t, \tau, \underline{U}) + A^3 \partial_u^2 G(t, \tau, \underline{U})(\Pi G(t, \tau, \underline{U}), \Pi G(t, \tau, \underline{U})) \\ &+ A^3 \partial_u G(t, \tau, \underline{U}) \Pi \partial_t G(t, \tau, \underline{U}) + A^3 \partial_u G(t, \tau, \underline{U}) \Pi \partial_u G(t, \tau, \underline{U}) \Pi G(t, \tau, \underline{U}). \end{aligned}$$

Since  $\Pi$  and  $A$  are bounded on  $C^0(\mathbb{T}_\tau; H^\sigma)$  for any  $\sigma$ , it follows that  $h_1, h_2, h_3 = \mathcal{O}(1)$  under suitable Sobolev norm, and this ensures the consistency of the ansatz (2.17) and the derivation process.

We now proceed to derive the complete initial value  $U(0, \tau, x)$ . Utilizing the Chapman-Enskog expansion (2.13) and (2.17) at the initial time, we obtain that

$$U(0, \tau, x) = \underline{U}(0) + \varepsilon^2 h_1(0, \tau, \underline{U}(0)) + \varepsilon^4 h_2(0, \tau, \underline{U}(0)) + \varepsilon^6 h_3(0, \tau, \underline{U}(0)) + \mathcal{O}(\varepsilon^8),$$

the initial data  $\underline{U}(0)$  will be determined such that it is consistent with the asymptotic order established above. By the initial restriction  $\Phi_0 = U(0, 0, x)$ , the proper  $\underline{U}(0)$  can be determined via an iterative procedure:

$$(2.20) \quad \underline{U}^{[0]} := \Phi_0, \quad \underline{U}^{[r]} = \Phi_0 - \sum_{l=1}^r \varepsilon^{2(r-l+1)} h_l(0, 0, \underline{U}^{[r-l]}), \quad r = 1, 2, 3, \quad \text{where } \underline{U}^{[r]} - \underline{U}(0) = \mathcal{O}(\varepsilon^{2(r+1)}).$$

Therefore, the complete set of initial conditions for the two-scale equation (2.12) is formulated as follows:

$$(2.21) \quad U(0, \tau, x) = \underline{U}^{[3]} + \varepsilon^2 h_1(0, \tau, \underline{U}^{[2]}) + \varepsilon^4 h_2(0, \tau, \underline{U}^{[1]}) + \varepsilon^6 h_3(0, \tau, \underline{U}^{[0]}) =: U_0(\tau, x), \quad \tau \in \mathbb{T}_\tau.$$

**2.3. Full discretization.** In this part, we present the full discretization. To begin, we employ the Fourier spectral method in the spatial  $x$  direction (as described in [52]) for solving (2.10). Choose the mesh size  $h := \Delta x = (b-a)/N_x$  with  $N_x$  a positive even integer, and denote grid points as  $x_j := a + jh$  for  $j = 0, 1, \dots, N_x$ . Specially, the first and second order Fourier differential matrices are introduced as

$$(2.22) \quad A_{kj}^{(1)} := \begin{cases} \frac{(-1)^{k+j}}{2} \cot\left(\frac{(k-j)\pi}{N_x}\right), & k \neq j, \\ 0, & k = j, \end{cases} \quad A_{kj}^{(2)} := \begin{cases} \frac{(-1)^{k+j}}{-2} \sin^{-2}\left(\frac{(k-j)\pi}{N_x}\right), & k \neq j, \\ \frac{N_x^2}{-12} - \frac{1}{6}, & k = j, \end{cases}$$

with  $k, j = 0, \dots, N_x - 1$ . Thence the operators  $\mathcal{D}^\varepsilon$  and  $\Pi_\pm$  are replaced by

$$\mathcal{D}_f^\varepsilon = \frac{1}{\varepsilon^2} \text{diag}\left((I - \varepsilon^2 A_{kj}^{(2)})^{1/2} - I, (I - \varepsilon^2 A_{kj}^{(2)})^{1/2} - I\right),$$

$$\Pi_{\pm, f}^\varepsilon = \frac{1}{2} \begin{pmatrix} I \pm (I - \varepsilon^2 A_{kj}^{(2)})^{-1/2} & \mp i\varepsilon A_{kj}^{(1)} (I - \varepsilon^2 A_{kj}^{(2)})^{-1/2} \\ \mp i\varepsilon A_{kj}^{(1)} (I - \varepsilon^2 A_{kj}^{(2)})^{-1/2} & I \mp (I - \varepsilon^2 A_{kj}^{(2)})^{-1/2} \end{pmatrix},$$

where  $I = I_{N_x \times N_x}$  is  $N_x \times N_x$  identity matrix,  $\mathcal{D}_f^\varepsilon$  and  $\Pi_{\pm, f}^\varepsilon$  are  $2 \times 2$  matrix blocks and each matrix block is an  $N_x \times N_x$  matrix. Then the system (2.10) can be discretized into the following ODEs:

$$(2.23) \quad \frac{d}{dt} W(t) = (e^{\frac{it}{\varepsilon^2}} e^{it\mathcal{D}_f^\varepsilon} \Pi_{+, f}^\varepsilon + e^{-\frac{it}{\varepsilon^2}} e^{-it\mathcal{D}_f^\varepsilon} \Pi_{-, f}^\varepsilon) \Lambda((e^{-\frac{it}{\varepsilon^2}} e^{-it\mathcal{D}_f^\varepsilon} \Pi_{+, f}^\varepsilon + e^{\frac{it}{\varepsilon^2}} e^{it\mathcal{D}_f^\varepsilon} \Pi_{-, f}^\varepsilon) W(t)),$$

where  $W(t) = [\psi_1(x_1, t), \dots, \psi_1(x_{N_x}, t), \psi_2(x_1, t), \dots, \psi_2(x_{N_x}, t)]^\top$ ,  $\Lambda(\Phi_f) = -i(V_f + \mathbf{F}(\Phi_f(t)))\Phi_f(t)$ , and  $V_f$  denotes the discrete set of potential values  $V(x_j)_{j=0,1,\dots,N_x-1}$  along the spatial grids.

For the system (2.23), according to Subsection 2.2, its two-scale form can be expressed as

$$(2.24) \quad \partial_t Z(t, \tau) + \frac{1}{\varepsilon^2} \partial_\tau Z(t, \tau) = \Upsilon(t, \tau, Z(t, \tau)),$$

with

$$\Upsilon(t, \tau, Z(t, \tau)) = (e^{i\tau} e^{it\mathcal{D}_f^\varepsilon} \Pi_{+, f}^\varepsilon + e^{-i\tau} e^{-it\mathcal{D}_f^\varepsilon} \Pi_{-, f}^\varepsilon) \Lambda((e^{-i\tau} e^{-it\mathcal{D}_f^\varepsilon} \Pi_{+, f}^\varepsilon + e^{i\tau} e^{it\mathcal{D}_f^\varepsilon} \Pi_{-, f}^\varepsilon) Z(t, \tau)).$$

When  $\tau = t/\varepsilon^2$ , it is obtained that  $Z(t, \tau) = W(t)$ . Let  $N_\tau$  be an even positive integer and define  $\Delta\tau = \frac{2\pi}{N_\tau}$ ,  $\tau_k = \frac{2\pi}{N_\tau} k$  with  $k = 0, 1, \dots, N_\tau - 1$ . For any periodic function  $v(\tau)$  on  $[0, 2\pi)$ , denote by  $P_{\mathcal{M}} : L^2([0, 2\pi)) \rightarrow Y_{\mathcal{M}}$  the standard projection operator  $(P_{\mathcal{M}}v)(\tau) = \sum_{l \in \mathcal{M}} \widehat{v}_l e^{il\tau}$  with  $l \in \mathcal{M} := \{-\frac{N_\tau}{2}, -\frac{N_\tau}{2} + 1, \dots, \frac{N_\tau}{2} - 1\}$  and by  $I_{\mathcal{M}} : C([0, 2\pi)) \rightarrow Y_{\mathcal{M}}$  the trigonometric interpolation operator  $(I_{\mathcal{M}}v)(\tau) = \sum_{l \in \mathcal{M}} \widetilde{v}_l e^{il\tau}$ , where  $\widehat{v}_l$  and  $\widetilde{v}_l$  are respectively defined as  $\widehat{v}_l = \frac{1}{2\pi} \int_0^{2\pi} v(\tau) e^{-il\tau} d\tau$  and  $\widetilde{v}_l = \frac{1}{N_\tau} \sum_{k=0}^{N_\tau-1} v(\tau_k) e^{-il\tau_k}$ . Then the Fourier spectral method is given in the  $\tau$  direction by finding the trigonometric polynomials  $Z^{\mathcal{M}}(t, \tau) = P_{\mathcal{M}}Z(t, \tau) = (Z_{1,j}^{\mathcal{M}}(t, \tau), Z_{2,j}^{\mathcal{M}}(t, \tau))_{j=1,2,\dots,N_x}$  such that

$$(2.25) \quad \partial_t Z^{\mathcal{M}}(t, \tau) + \frac{1}{\varepsilon^2} \partial_\tau Z^{\mathcal{M}}(t, \tau) = \Upsilon(t, \tau, Z^{\mathcal{M}}(t, \tau)).$$

Consider the notation  $\widehat{\mathbf{Z}} = [\widehat{\mathbf{Z}}_1; \widehat{\mathbf{Z}}_2]$  with  $\widehat{\mathbf{Z}}_m := (\widehat{Z}_{m,j}^l)_{j=1,2,\dots,N_x, l \in \mathcal{M}}$  for  $m = 1, 2$ , where  $(\widehat{Z}_{m,j}^l)_{l \in \mathcal{M}}$  are the Fourier coefficients of  $Z_{m,j}^{\mathcal{M}}$ . Then, we obtain

$$(2.26) \quad \frac{d}{dt} \widehat{\mathbf{Z}}(t) = i\Theta \widehat{\mathbf{Z}}(t) + \Xi(t, \widehat{\mathbf{Z}}(t)),$$

where  $\widehat{\mathbf{Z}}$  is a  $2N_x \times N_\tau$  dimensional vector,  $\Theta := \text{diag}(\Theta_1, \Theta_2, \dots, \Theta_{2N_x})$  with  $\Theta_1 = \Theta_2 = \dots = \Theta_{2N_x} := \frac{1}{\varepsilon^2} \text{diag}\left(\frac{N_\tau}{2}, \frac{N_\tau}{2} - 1, \dots, -\frac{N_\tau}{2} + 1\right)$  and

$$(2.27) \quad \Xi(t, \widehat{\mathbf{Z}}) = \mathfrak{F}\left((-i)\mathcal{C}_- \left(V_f + F(\mathcal{C}_+ \mathfrak{F}^{-1} \widehat{\mathbf{Z}})\right) (\mathcal{C}_+ \mathfrak{F}^{-1} \widehat{\mathbf{Z}})\right).$$

Here  $\mathfrak{F}$  denotes the discrete Fast Fourier Transform (FFT), and

$$\mathcal{C}_{\pm} := \text{diag} \left( e^{\mp i \tau_k} e^{\mp i t \mathcal{D}_f^{\varepsilon}} \Pi_{+,f}^{\varepsilon} + e^{\pm i \tau_k} e^{\pm i t \mathcal{D}_f^{\varepsilon}} \Pi_{-,f}^{\varepsilon} \right)_{k=0,1,\dots,N_{\tau}-1}.$$

Based on the Duhamel formula for (2.26)

$$(2.28) \quad \widehat{\mathbf{Z}}(t_n + \xi) = e^{\xi i \Theta} \widehat{\mathbf{Z}}(t_n) + \int_0^{\xi} e^{(\xi-\theta) i \Theta} \Xi(t_n + \theta, \widehat{\mathbf{Z}}(t_n + \theta)) d\theta, \quad 0 \leq \xi \leq \Delta t, \quad n \geq 0,$$

we adopt the framework of the  $s$ -stage exponential integrator ([39, 40]):

$$(2.29) \quad \begin{aligned} \widehat{\mathbf{Z}}^{n,j} &= e^{c_j i \Theta \Delta t} \widehat{\mathbf{Z}}^n + \Delta t \sum_{k=1}^s a_{jk} (i \Theta \Delta t) \Xi(t_n + c_k \Delta t, \widehat{\mathbf{Q}}^{n,k}), \quad j = 1, 2, \dots, s, \\ \widehat{\mathbf{Z}}^{n+1} &= e^{i \Theta \Delta t} \widehat{\mathbf{Z}}^n + \Delta t \sum_{j=1}^s b_j (i \Theta \Delta t) \Xi(t_n + c_j \Delta t, \widehat{\mathbf{Q}}^{n,j}), \quad n \geq 0, \end{aligned}$$

where  $\Delta t$  is a time stepsize,  $c_j \in [0, 1]$  and  $a_{jk}(z), b_j(z)$  are bounded coefficient functions of  $z \in \mathbb{C}$  for  $j, k = 1, 2, \dots, s$  and  $s \in \mathbb{N}_+$ . If the coefficients satisfy the following conditions:

$$(2.30) \quad c_{\rho} = 1 - c_{s+1-\rho}, \quad b_{\rho}(z) = e^z b_{s+1-\rho}(-z), \quad a_{j\rho}(z) = e^{c_j z} b_{s+1-\rho}(-z) - a_{s+1-j, s+1-\rho}(-z),$$

where  $\rho, j = 1, 2, \dots, s$ , then the integrator (2.29) is time symmetric.

Based on these symmetry conditions and the stiff order conditions of exponential integrators ([39, 40]), we construct the following two numerical schemes, which will be proved to have fourth-order accuracy in the next section.

• **Symmetric scheme** We consider  $s = 3$  and choose the following coefficients

$$(2.31) \quad \begin{aligned} a_{31} &= a_{32} = a_{33} = 0, \quad a_{21} = -\frac{1}{4}\varphi_{2,2} + \frac{1}{2}\varphi_{3,2}, \quad a_{22} = \varphi_{2,2} - \varphi_{3,2}, \quad a_{23} = \frac{1}{2}\varphi_{1,2} - \frac{3}{4}\varphi_{2,2} + \frac{1}{2}\varphi_{3,2}, \\ a_{11} &= b_1 = 4\varphi_3 - \varphi_2, \quad a_{12} = b_2 = 4\varphi_2 - 8\varphi_3, \quad a_{13} = b_3 = \varphi_1 - 3\varphi_2 + 4\varphi_3, \end{aligned}$$

where  $\varphi_{i,j} = \varphi_{i,j}(i\Theta\Delta t) = \varphi_i(c_j i\Theta\Delta t)$  with  $\varphi_{\rho}(z) := \int_0^1 \theta^{\rho-1} \frac{e^{(1-\theta)z}}{(\rho-1)!} d\theta$ . This scheme is symmetric and we denote it by SEP-TS4.

• **Explicit scheme** Now we consider explicit schemes and the coefficients are given as

$$(2.32) \quad \begin{aligned} c_1 &= 0, \quad c_2 = c_3 = c_5 = \frac{1}{2}, \quad c_4 = 1, \quad a_{2,1} = \frac{1}{2}\varphi_{1,2}, \quad a_{3,1} = \frac{1}{2}\varphi_{1,3} - \varphi_{2,3}, \quad a_{3,2} = \varphi_{2,3}, \\ a_{4,1} &= \varphi_{1,4} - 2\varphi_{2,4}, \quad a_{4,2} = a_{4,3} = \varphi_{2,4}, \quad a_{5,1} = \frac{1}{2}\varphi_{1,5} - 2a_{5,2} - a_{5,4}, \\ a_{5,2} &= \frac{1}{2}\varphi_{2,5} - \varphi_{3,4} + \frac{1}{2}\varphi_{2,4} - \frac{1}{2}\varphi_{3,5}, \quad a_{5,3} = a_{5,2}, \quad a_{5,4} = \frac{1}{4}\varphi_{2,5} - \varphi_{5,2}, \\ b_1 &= \varphi_1 - 3\varphi_2 + 4\varphi_3, \quad b_2 = b_3 = 0, \quad b_4 = -\varphi_2 + 4\varphi_3, \quad b_5 = 4\varphi_2 - 8\varphi_3. \end{aligned}$$

This scheme is not symmetric but is explicit. It is referred as EEP-TS4.

Based on the preceding derivations, we are now prepared to introduce the fully discrete integrators for solving the original Dirac equation (1.1).

**DEFINITION 2.1. (Fully discrete integrators)** For the nonlinear Dirac equation (1.1) in the nonrelativistic regime, choosing the time step size  $\Delta t$ , positive even number  $N_x$  and  $N_{\tau}$ , then the SEP-TS4 & EEP-TS4 integrators are defined as follows.

- Derive the fourth order initial data  $Z(0, \tau)$  by inputting  $\Phi_0$  into (2.21) and then set  $\widehat{\mathbf{Z}}^0 = [\widehat{\mathbf{Z}}_1^0; \widehat{\mathbf{Z}}_2^0] := \text{FFT}((Z^0(\tau_k))_{k=0,1,\dots,N_{\tau}-1})$ .
- Compute  $\widehat{\mathbf{Z}}^{n+1}$  using EP-TS4 schemes (2.29) with coefficients (2.31) or (2.32), for  $n = 0, 1, \dots, T/\Delta t - 1$ .



**Algorithm 2.1** Pseudo-code of fully discrete integrators for the NLDE (1.1)**Input:** Initial value  $\Phi_0(x)$ ; Time stepsize  $\Delta t$ ; End time  $T$ .**Output:** Numerical solution  $\Phi^{n+1}(x) \approx \Phi((n+1)\Delta t, x)$ ,  $n = 0 : \frac{T}{\Delta t} - 1$ .

---

```

1:  $\underline{U}^{[0]}(x_j) = \Phi_0(x_j)_{j=0,1,\dots,N_x-1}$ 
2: for  $r = 1 : 3$  do
3:    $\underline{U}^{[r]} = \Phi_0 - \sum_{l=1}^r \varepsilon^{2(r-l+1)} h_l(0, 0, \underline{U}^{[r-l]}).$ 
4: end for
5:  $U(0, \tau, x_j) = \underline{U}^{[3]} + \varepsilon^2 h_1(0, \tau, \underline{U}^{[2]}) + \varepsilon^4 h_2(0, \tau, \underline{U}^{[1]}) + \varepsilon^6 h_3(0, \tau, \underline{U}^{[0]}).$ 
6:  $Z^0(\tau) = (U_0(\tau, x_j))_{j=0,1,\dots,N_x-1}$  % the initial value of the equation (2.24)
7:  $\hat{\mathbf{Z}}^0 := \text{FFT}\left((Z^0(\tau_k))_{k=0,1,\dots,N_\tau-1}\right)$  % the initial value of the equation (2.26)
8: for  $n = 0 : \frac{T}{\Delta t} - 1$  do
9:   for  $j = 1 : s$  ( $s = 3, 5$ ) do
10:     $\hat{\mathbf{Z}}^{n,j} = e^{c_j i \Theta \Delta t} \hat{\mathbf{Z}}^n + \Delta t \sum_{k=1}^s a_{jk}(i \Theta \Delta t) \Xi(t_n + c_k \Delta t, \hat{Q}^{n,k}).$ 
11:   end for
12:    $\hat{\mathbf{Z}}^{n+1} = e^{i \Theta \Delta t} \hat{\mathbf{Z}}^n + \Delta t \sum_{j=1}^s b_j(i \Theta \Delta t) \Xi(t_n + c_j \Delta t, \hat{Q}^{n,j}).$ 
13:    $\Phi^{n+1} = e^{\frac{-i(n+1)\Delta t}{\varepsilon^2} Q^\varepsilon} Z^{n+1}((n+1)\Delta t/\varepsilon^2).$ 
14: end for

```

---

- Then the numerical solution  $\Phi^{n+1} \approx \Phi(t_{n+1}, x)$  of the NLDE (1.1) is formulated as

$$(2.33) \quad \Phi^{n+1} = e^{-\frac{it_{n+1}}{\varepsilon^2} Q^\varepsilon} Z^{n+1}, \quad n = 0, 1, \dots, T/\Delta t - 1,$$

where  $Z^{n+1}$  is obtained by  $Z^{n+1} = \sum_{l \in \mathcal{M}} (\hat{\mathbf{Z}}^{n+1})_l e^{il t_{n+1}/\varepsilon^2}$ .

The details of the whole procedure are given in **Algorithm 2.1**.

In practice, the integrals appeared in the computing Fourier transform coefficients are not suitable. Consequently, the scheme (2.29) is typically replaced by interpolation schemes in practical computations. Choosing  $\mathbf{Z}^0 = (Z^0(\tau_k))_{k=0,1,\dots,N_\tau-1}$ , then the Fourier pseudospectral (FP) discretization reads

$$(2.34) \quad Z^{n+1}(\tau) = \sum_{l \in \mathcal{M}} (\tilde{\mathbf{Z}}^{n+1})_l e^{il \tau},$$

where

$$(2.35) \quad \begin{aligned} \tilde{\mathbf{Z}}^{n,j} &= e^{c_j i \Theta \Delta t} \tilde{\mathbf{Z}}^n + \Delta t \sum_{k=1}^s a_{jk}(i \Theta \Delta t) \Xi(t_n + c_k \Delta t, \tilde{\mathbf{Z}}^{n,k}), \quad j = 1, 2, \dots, s, \\ \tilde{\mathbf{Z}}^{n+1} &= e^{i \Theta \Delta t} \tilde{\mathbf{Z}}^n + \Delta t \sum_{j=1}^s b_j(i \Theta \Delta t) \Xi(t_n + c_j \Delta t, \tilde{\mathbf{Z}}^{n,j}), \quad n \geq 0, \end{aligned}$$

with the coefficients (2.31) or (2.32).

**3. Uniform accuracy and long-time analysis.** In this section, we shall study the uniform accuracy and long-time behaviour of the proposed integrators.

**3.1. Error estimates.** In order to obtain the error bounds for the integrators (2.29), we assume that the electric potential and the exact solution to the NLDE (2.7) satisfies:

$$\|V\|_{W_p^{\nu+m_0,\infty}} \lesssim 1, \quad \|\Phi\|_{L^\infty([0,T];(H_p^{\nu+m_0})^2)} \lesssim 1,$$

where  $\nu > d/2 + 8$ ,  $m_0 \geq 1$ , and  $W_p^{m,\infty} = \{u | u \in W^{m,\infty}(\Omega), \partial_x^l u(a) = \partial_x^l u(b), l = 0, \dots, m-1\}$ ,  $H_p^m(\Omega) = \{u | u \in H^m(\Omega), \partial_x^l u(a) = \partial_x^l u(b), l = 0, \dots, m-1\}$  for  $m \in \mathbb{N}$ . For simplicity, in this section we use  $A \lesssim B$  to denote that there exists a generic constant  $C > 0$  independent of  $\varepsilon, \Delta t, \Delta x, \Delta \tau$  such that  $A \leq CB$ .



**THEOREM 3.1. (*Uniform accuracy*)** Under the assumptions stated above, there exist  $t_0 > 0$ ,  $h_0 > 0$  and  $\tau_0 > 0$  independent of  $\varepsilon$  such that for any  $0 < \varepsilon \leq 1$ , when  $0 < \Delta t \leq t_0$ ,  $0 < \Delta x \leq h_0$  and  $0 < \Delta \tau \leq \tau_0$ , the global errors  $e_\Phi^n := \Phi(t_n, \cdot) - \Phi^n$  of fully discrete integrators are bounded by

$$(3.1) \quad \|e_\Phi^n\|_{H^1} \lesssim \Delta t^4 + \Delta x^{m_0} + \Delta \tau^{\nu-1}, \quad n = 0, 1, \dots, T/\Delta t,$$

where  $\nu > 8 + d/2$  and  $m_0 \geq 1$ .

*Remark 3.2.* The error estimates in Theorem 3.1 also hold for the scheme (2.34)-(2.35), and the proof follows a similar way as given in [28, 55].

*Proof.* Here we only prove the global error of the SEP-TS4 integrator, and the proof of EEP-TS4 scheme is similar.

The property of two-scale differential equation will be used in the error analysis and we first study this aspect. In an analogous way as in [23, 46], the solution of the two-scale system (2.12) with the initial value (2.21) can be estimated as

$$\|U(t, \tau, x)\|_{L_\tau^\infty(H^{\nu+m_0})} \leq C, \quad \forall t \in [0, T],$$

where the constant  $C > 0$  depends on  $\|\Phi_0\|_{L_\tau^\infty(H^{\nu+m_0})}$  but is independent of  $\varepsilon$ . Moreover, the derivatives of  $U$  w.r.t.  $t$  are bounded as

$$(3.2) \quad \|\partial_t^k U(t, \tau, \cdot)\|_{L_\tau^\infty(H^{\nu+m_0-2k})} \leq C, \quad \forall t \in [0, T], \quad k = 1, 2, 3, 4.$$

Then we study the error brought by the Fourier spectral method in the spatial  $x$ . By estimates on projection error [52], we can obtain that

$$\|\Psi(t_n, x) - W(t_n)\|_{H^\nu} \lesssim \Delta x^{m_0}.$$

In order to study the error brought by Fourier spectral method on  $\tau$ , define the error function by

$$e_Z^n(\tau) := Z(t_n, \tau) - P_{\mathcal{M}}Z^n$$

and the projected error as

$$e_{\mathcal{M}}^n(\tau) := P_{\mathcal{M}}Z(t_n, \tau) - Z_{\mathcal{M}}^n(\tau),$$

where we use the notation  $Z_{\mathcal{M}}^{n+1}(\tau) = \sum_{l \in \mathcal{M}} (\widehat{Z}^{n+1})_l e^{il\tau}$ . Since  $Z(t_n, \tau)$  is an argumented function of  $W(t_n)$  and  $\|W(t_n)\|_{H^\nu} = \|Z(t_n, t_n/\varepsilon^2)\|_{H^\nu}$ , which implies that  $Z(t_n, \tau) \in H^\nu$ . By applying the triangle inequality and estimates on projection error, we obtain that

$$(3.3) \quad \|e_Z^n\|_{H^1} \leq \|e_{\mathcal{M}}^n\|_{H^1} + \|Z(t_n, \tau) - P_{\mathcal{M}}Z(t_n, \tau)\|_{H^1} \lesssim \|e_{\mathcal{M}}^n\|_{H^1} + \Delta \tau^{\nu-1}.$$

Based on the transformation of the equation and the formulation of integrators, we get

$$(3.4) \quad \begin{aligned} \|e_\Phi^n\|_{H^1} &= \|\Phi(t_n, \cdot) - \Phi^n\|_{H^1} = \left\| e^{\frac{-it_n}{\varepsilon^2} Q^\varepsilon} \Psi(t_n, \cdot) - e^{\frac{-it_n}{\varepsilon^2} Q^\varepsilon} P_{\mathcal{M}}Z^n \right\|_{H^1} \\ &\lesssim \|\Psi(t_n, \cdot) - P_{\mathcal{M}}Z^n\|_{H^1} \\ &= \|\Psi(t_n, \cdot) - W(t_n) + W(t_n) - Z(t_n, t_n/\varepsilon^2) + Z(t_n, t_n/\varepsilon^2) - P_{\mathcal{M}}Z^n\|_{H^1} \\ &\leq \|\Psi(t_n, \cdot) - W(t_n)\|_{H^1} + \|e_Z^n\|_{H^1} \leq \|\Psi(t_n, \cdot) - W(t_n)\|_{H^\nu} + \|e_Z^n\|_{H^1} \\ &\lesssim \|e_{\mathcal{M}}^n\|_{H^1} + \Delta x^{m_0} + \Delta \tau^{\nu-1}. \end{aligned}$$

Therefore, the estimate of error  $e_\Phi^n$  is converted to the estimate of error  $e_{\mathcal{M}}^n$ .

For the error  $e_{\mathcal{M}}^n(\tau) = P_{\mathcal{M}}Z(t_n, \tau) - Z_{\mathcal{M}}^n(\tau) = \sum_{l \in \mathcal{M}} (\widehat{Z}(t_n) - \widehat{Z}^n)_l e^{il\tau}$ , we need to study the error  $\widehat{\mathbf{Z}}(t_n) - \widehat{\mathbf{Z}}^n$ . In order to simplify the notation, we set  $\widehat{\Gamma}(t) = \Xi(t, \widehat{\mathbf{Z}}(t))$ . Substituting the solution of (2.26) into (2.29), we write

$$(3.5) \quad \begin{aligned} \widehat{\mathbf{Z}}(t_n + c_j \Delta t) &= e^{c_j i \Theta \Delta t} \widehat{\mathbf{Z}}(t_n) + \Delta t \sum_{k=1}^3 a_{jk} (i \Theta \Delta t) \widehat{\Gamma}(t_n + c_k \Delta t) + \delta^{n,j}, \\ \widehat{\mathbf{Z}}(t_{n+1}) &= e^{i \Theta \Delta t} \widehat{\mathbf{Z}}(t_n) + \Delta t \sum_{j=1}^3 b_j (i \Theta \Delta t) \widehat{\Gamma}(t_n + c_j \Delta t) + \delta^{n+1}, \end{aligned}$$

where  $\delta^{n,j}$  and  $\delta^{n+1}$  denote the remainders for  $j = 1, 2, 3$  and  $n = 0, 1, \dots, T/\Delta t$ . Define

$$\Psi_\rho(z) := \varphi_\rho(z) - \sum_{j=1}^3 b_j(z) \frac{c_j^{\rho-1}}{(\rho-1)!}, \quad \Psi_{\rho,j}(z) := \varphi_\rho(c_j z) c_j^\rho - \sum_{k=1}^3 a_{jk}(z) \frac{c_k^{\rho-1}}{(\rho-1)!},$$

for  $j = 1, 2, 3$  and  $\rho = 1, 2, \dots$ . Subtracting (3.5) from (2.28) with  $\xi = \Delta t$  and applying the Taylor expansion to  $\widehat{\Gamma}(t)$ ,  $\delta^{n+1}$  can be derived as

$$\begin{aligned} \delta^{n+1} &= \Delta t \int_0^1 e^{(1-\theta)\mathbf{i}\Theta\Delta t} \sum_{\rho=1}^4 \frac{(\theta\Delta t)^{\rho-1}}{(\rho-1)!} \frac{d^{\rho-1}}{dt^{\rho-1}} \widehat{\Gamma}(t_n) d\theta \\ &\quad - \Delta t \sum_{j=1}^3 b_j(\mathbf{i}\Theta\Delta t) \sum_{\rho=1}^4 \frac{c_j^{\rho-1} \Delta t^{\rho-1}}{(\rho-1)!} \frac{d^{\rho-1}}{dt^{\rho-1}} \widehat{\Gamma}(t_n) + \widetilde{\delta_4^{n+1}} \\ &= \sum_{\rho=1}^4 \Delta t^\rho \Psi_\rho(\mathbf{i}\Theta\Delta t) \frac{d^{\rho-1}}{dt^{\rho-1}} \widehat{\Gamma}(t_n) + \widetilde{\delta_4^{n+1}}. \end{aligned} \tag{3.6}$$

Here,  $\widetilde{\delta_4^{n+1}}$  represents the truncation error of the Taylor expansions, which is bounded as  $\widetilde{\delta_4^{n+1}} = \mathcal{O}(\Delta t^5)$  based on (3.2). Using the choice (2.31), it is easy to check that  $\Psi_\rho = 0$  for  $\rho = 1, 2, 3, 4$ . Thus one gets

$$\delta^{n+1} = \widetilde{\delta_4^{n+1}} = \mathcal{O}(\Delta t^5).$$

Similarly, analogous results can be derived as

$$\delta^{n,j} = \sum_{\rho=1}^3 \Delta t^\rho \Psi_{\rho,j}(\mathbf{i}\Theta\Delta t) \frac{d^{\rho-1}}{dt^{\rho-1}} \widehat{\Gamma}(t_n) + \widetilde{\delta_3^{n,j}} = \widetilde{\delta_3^{n,j}}$$

with  $\widetilde{\delta_3^{n,j}} = \mathcal{O}(\Delta t^4)$ . Following the similar error estimates of exponential integrators, we can get that the time error is

$$\left\| \widehat{\mathbf{Z}}(t_n) - \widehat{\mathbf{Z}}^n \right\|_{H^1} \lesssim \Delta t^4.$$

This, together with equation (3.4), gives the global error (3.1).  $\square$

**3.2. Long-time analysis.** Now we turn to the long-time analysis and to this end, consider the notations (see [46]):

$$\begin{aligned} \mathbf{k} &= \left( k_{-\frac{N_x}{2},1}, \dots, k_{\frac{N_x}{2}-1,1}, k_{-\frac{N_x}{2},2}, \dots, k_{\frac{N_x}{2}-1,2}, \dots, k_{-\frac{N_x}{2},2N_x}, \dots, k_{\frac{N_x}{2}-1,2N_x} \right), \\ |\mathbf{k}| &= \sum_{l=1}^{2N_x} \sum_{j=-N_x/2}^{N_x/2-1} |k_{j,l}|, \quad \boldsymbol{\omega} = (\text{diagonal elements of } \Theta), \quad \mathbf{k} \cdot \boldsymbol{\omega} = \sum_{l=1}^{2N_x} \sum_{j=-N_x/2}^{N_x/2-1} k_{j,l} \omega_{j,l}. \end{aligned}$$

Using the notation  $\mathcal{Q} = \{\mathbf{k} \in \mathbb{Z}^D : \text{there exists an } l \in \{1, \dots, 2N_x\} \text{ such that } |\mathbf{k}_{:,l}| = |\mathbf{k}|\}$ , we define the resonance module  $\mathcal{M} = \{\mathbf{k} \in \mathcal{Q} : \mathbf{k} \cdot \boldsymbol{\omega} = 0\}$ . Let  $\mathcal{K}$  represent a set of representatives for the equivalence classes in  $\mathcal{Q}/\mathcal{M}$ , selected such that for every  $\mathbf{k} \in \mathcal{K}$ , the sum  $|\mathbf{k}|$  is the smallest within its equivalence class  $[\mathbf{k}] = \mathbf{k} + \mathcal{M}$ , and it is also required that  $-\mathbf{k} \in \mathcal{K}$ . For any integer  $N > 0$ , we introduce the following notation:

$$(3.7) \quad \mathcal{N}_N = \{\mathbf{k} \in \mathcal{K} : |\mathbf{k}| \leq N\}, \quad \mathcal{N}_N^* = \mathcal{N} \cup \{\langle 0 \rangle_l\}_{l=1,2,\dots,2N_x},$$

where  $\langle j \rangle_l$  is the unit coordinate vector in  $\mathbb{R}^D$ , represented as  $(0, \dots, 0, 1, 0, \dots, 0)^\top$  with the sole non-zero entry of 1 located at the  $(j, l)$ -th position. Further details on these notations can be found in [46].

**THEOREM 3.3. (Long time near conservations)** *For the initial value (2.21) of the two-scale equation (2.12), it is assumed to have the bound  $0 < \delta_0 := \|\Phi_0\|_{L^\infty_\tau(H^{\nu+m_0})} < 1$ . Moreover, we assume the following non-resonance requirement  $|\sin(\frac{1}{2}\Delta t \omega_{j,1})| \geq c_1 \sqrt{\varepsilon}$  for  $j = -\frac{N_\tau}{2}, -\frac{N_\tau}{2} + 1, \dots, \frac{N_\tau}{2} - 1$ , and the condition on the time stepsize:  $\Delta t / \sqrt{\varepsilon} \geq c_2 > 0$ . The symmetric numerical approximation (2.33) produced by SEP-TS4 has the following time near conservations*

$$(3.8) \quad \frac{\varepsilon^2}{\delta_0^2} |E(\Phi^n) - E(\Phi^0)| = \mathcal{O}(\varepsilon^2 \delta_0^4) + \mathcal{O}(\delta_{\mathcal{F}}), \quad \frac{1}{\delta_0^2} |M(\Phi^n) - M(\Phi^0)| = \mathcal{O}(\varepsilon^2 \delta_0^4) + \mathcal{O}(\delta_{\mathcal{F}}),$$

where  $0 \leq n\Delta t \leq \varepsilon^{-2} \delta_0^{-N+5}$ ,  $N$  is an arbitrarily large integer given in (3.7),  $\mathcal{O}$  denotes the term whose Euclidean norm is bounded, and  $\delta_{\mathcal{F}}$  denotes the error brought by the Fourier pseudospectral discretizations in  $x$  and  $\tau$ . The constants symbolized by  $\mathcal{O}$  can depend on  $c_1, c_2, N, N_\tau, N_x$  but are independent of  $n, \Delta t, \varepsilon, \delta_0$ .

*Proof.* This result is established within the framework of modulated Fourier expansion (MFE) [36, 37, 55]. The proof is provided for the energy conservation property and the derivation for mass conservation follows similarly.

We initially seek the modulated Fourier expansion (MFE) of the numerical solution  $\hat{\mathbf{Z}}^n$  produced by (2.29):

$$(3.9) \quad \hat{\mathbf{Z}}^n = \Phi_{\text{MFE}}(t) := \sum_{\mathbf{k} \in \mathcal{N}_\infty^*} e^{i(\mathbf{k} \cdot \boldsymbol{\omega})t} \alpha^{\mathbf{k}}(t), \quad t = n\Delta t,$$

where  $\mathcal{N}_\infty^*$  represents the limit of  $\mathcal{N}_N^*$  as  $N \rightarrow +\infty$ . Analogous to the analysis of local errors, we demonstrate that the error between  $\hat{\mathbf{Z}}^{n,j}$  and  $\Phi_{\text{MFE}}(t + c_i \Delta t)$  is bounded by  $\mathcal{O}(\Delta t^5) \Phi_{\text{MFE}}^{(4)}(t + \theta_i \Delta t)$  for some  $\theta_i \in [0, c_i]$  and  $i = 1, 2, 3$ . Consequently, one has

$$\hat{\mathbf{Z}}^{n,i} = \Phi_{\text{MFE}}(t + c_i \Delta t) + C \Delta t^5 \mathcal{D}^4 \Phi_{\text{MFE}}(t + \theta_i \Delta t), \quad i = 1, 2, 3,$$

where  $C$  denotes an error constant that is independent of  $n, \Delta t, \varepsilon$ , and  $\mathcal{D}$  represents the differential operator as [37].

Upon substituting (3.9) into (2.29) and introducing the operator  $\mathcal{L}$

$$\begin{aligned} \mathcal{L}(\Delta t \mathcal{D}) := & \left( e^{\Delta t \mathcal{D}} - e^{i\Theta \Delta t} \right) \left( b_1(i\Theta \Delta t)(e^{c_1 \Delta t \mathcal{D}} + C \Delta t^5 \mathcal{D}^4 e^{\theta_1 \Delta t \mathcal{D}}) + b_2(i\Theta \Delta t) \right. \\ & \left. (e^{c_2 \Delta t \mathcal{D}} + C \Delta t^5 \mathcal{D}^4 e^{\theta_2 \Delta t \mathcal{D}}) + b_3(i\Theta \Delta t)(e^{c_3 \Delta t \mathcal{D}} + C \Delta t^5 \mathcal{D}^4 e^{\theta_3 \Delta t \mathcal{D}}) \right)^{-1}, \end{aligned}$$

we obtain  $\mathcal{L}(\Delta t \mathcal{D}) \Phi_{\text{MFE}}(t) = \Delta t f(\Phi_{\text{MFE}})$ , where  $f(\Phi_{\text{MFE}}) = \Xi(t, \Phi_{\text{MFE}})$ . By expanding the nonlinear term into its Taylor series, we derive

$$\mathcal{L}(\Delta t \mathcal{D}) \Phi_{\text{MFE}}(t) = \Delta t \sum_{\mathbf{k} \in \mathcal{N}_\infty^*} e^{i(\mathbf{k} \cdot \boldsymbol{\omega})t} \sum_{m \geq 1} \frac{f^{(m)}(0)}{m!} \sum_{\mathbf{k}^1 + \dots + \mathbf{k}^m = \mathbf{k}} \left[ \alpha^{\mathbf{k}^1} \dots \alpha^{\mathbf{k}^m} \right](t).$$

In the subsequent development, we establish the modulation system for the coefficients  $\alpha^{\mathbf{k}}(t)$ . This is accomplished by substituting the ansatz given in (3.9) into the relevant expressions and equating the coefficients associated with  $e^{i(\mathbf{k} \cdot \boldsymbol{\omega})t}$ . Consequently, we arrive at the following results:

$$\mathcal{L}(\Delta t \mathcal{D} + i(\mathbf{k} \cdot \boldsymbol{\omega})\Delta t) \alpha^{\mathbf{k}}(t) = \Delta t \sum_{m \geq 1} \frac{f^{(m)}(0)}{m!} \sum_{\mathbf{k}^1 + \dots + \mathbf{k}^m = \mathbf{k}} \left[ \alpha^{\mathbf{k}^1} \dots \alpha^{\mathbf{k}^m} \right](t).$$

This constitutes the modulation system for the coefficients  $\alpha^{\mathbf{k}}(t)$  of the modulated Fourier expansion (MFE). Based on this result and similar arguments given in [36, 37, 55], we demonstrate that the numerical solution derived from the SEP-TS4 scheme can be represented by

$$(3.10) \quad \hat{\mathbf{Z}}^n = \sum_{\mathbf{k} \in \mathcal{N}_N^*} e^{i(\mathbf{k} \cdot \boldsymbol{\omega})t} \alpha^{\mathbf{k}}(t) + R_N(t),$$

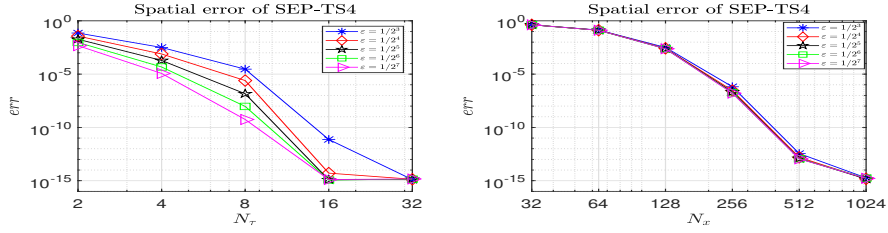


FIG. 2. *Problem 1. Spatial error of NLDE (1.1) in 1D at  $t = 1$  under different  $\varepsilon$  in  $\tau$ -direction (left) and in  $x$ -direction (right).*

where  $\alpha^{\mathbf{k}}$  are smooth coefficient functions at  $t = n\Delta t$  and the term  $R_N(t)$  represents the remainder resulting from the truncation process. The coefficient functions  $\alpha^{\mathbf{k}}$  are bounded by

$$(3.11) \quad \alpha_{j,l}^{(j)l}(t) = \mathcal{O}(\delta_0), \quad \dot{\alpha}_{j,l}^{(j)l}(t) = \mathcal{O}(\varepsilon^{5/2}\delta_0), \quad \alpha_{j,l}^{\mathbf{k}}(t) = \mathcal{O}(\varepsilon^2 \min(\delta_0^{|\mathbf{k}|}, \delta_0^3)), \quad \mathbf{k} \neq \langle j \rangle_l,$$

where  $j \in \{-N_\tau/2, -N_\tau/2 + 1, \dots, N_\tau/2 - 1\}$  and  $l = 1, 2, \dots, 2N_x$ . Standard convergence estimates (similar to the proof of Theorem 3.1) yield a bound for the remainder term  $R_N$ :

$$(3.12) \quad R_N(t) = \mathcal{O}(t\varepsilon^2\delta_0^{N+1}).$$

The construction of the coefficients  $\alpha^{\mathbf{k}}$  along with the remainder bound given by (3.12) yields an almost-invariant quantity. Furthermore, this almost-invariant is demonstrated to closely approximate the energy (1.5), with the magnitude of the discrepancy governed by the bound (3.11) on  $\alpha^{\mathbf{k}}$ . The analysis of this aspect is similar to that of [46, 54], and hence we only state the results here.

The synthesis of  $\alpha^{\mathbf{k}}$  gives rise to an almost-invariant  $\mathcal{H}(t)$ , which exhibits small variation as it evolves from 0 to  $t$

$$\mathcal{H}(t) = \mathcal{H}(0) + \mathcal{O}(t\varepsilon^2\delta_0^{N+1}).$$

Furthermore, this almost-invariant is closely aligned with the energy  $E$ , and their relationship is given by

$$\mathcal{H}(t_n) = E(\Phi^n) + \mathcal{O}(\delta_0^6) + \mathcal{O}(\delta_{\mathcal{F}}).$$

Having established the preceding preparations, we are now in a position to deduce the error in energy conservation.

$$\begin{aligned} E(\Phi^n) &= \mathcal{H}(t_n) + \mathcal{O}(\delta_0^6) + \mathcal{O}(\delta_{\mathcal{F}}) = \mathcal{H}(t_{n-1}) + \Delta t \mathcal{O}(\varepsilon^2\delta_0^{N+1}) + \mathcal{O}(\delta_0^6) + \mathcal{O}(\delta_{\mathcal{F}}) \\ &= \mathcal{H}(t_{n-2}) + 2\Delta t \mathcal{O}(\varepsilon^2\delta_0^{N+1}) + \mathcal{O}(\delta_0^6) + \mathcal{O}(\delta_{\mathcal{F}}) = \dots \\ &= \mathcal{H}(t_0) + n\Delta t \mathcal{O}(\varepsilon^2\delta_0^{N+1}) + \mathcal{O}(\delta_0^6) + \mathcal{O}(\delta_{\mathcal{F}}) = E(\Phi^0) + \mathcal{O}(\delta_0^6) + \mathcal{O}(\delta_{\mathcal{F}}), \end{aligned}$$

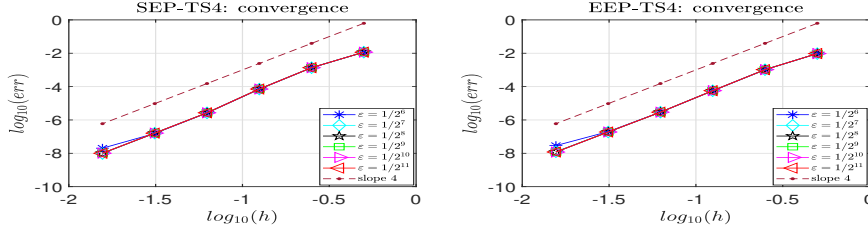
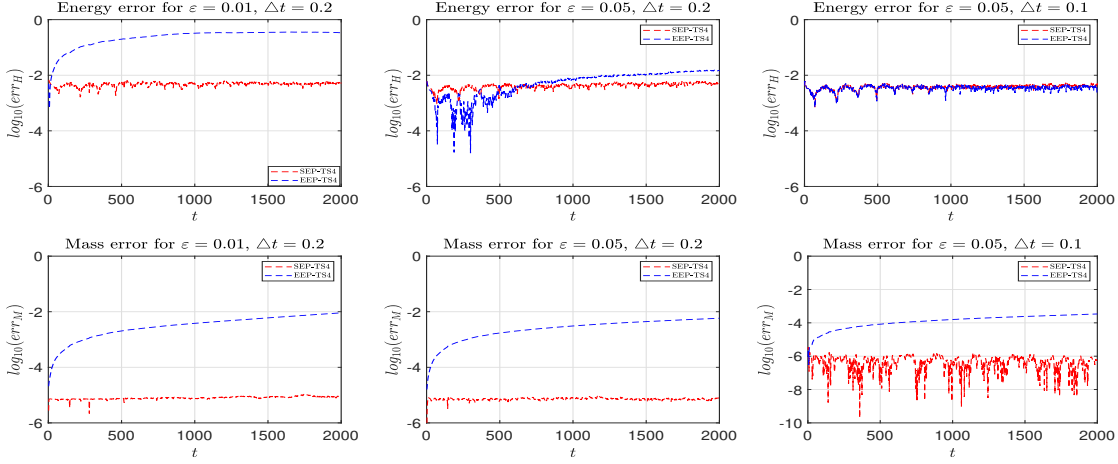
as long as  $n\Delta t\varepsilon^2\delta_0^{N+1} \leq \delta_0^6$ . The demonstration of the nearly conserved energy is thereby concluded.  $\square$

**4. Numerical experiments.** In this section, we apply the proposed two fourth order uniformly accurate integrators to different kinds of Dirac equation. We will test the accuracy and long-term energy and mass performance of each integrator.

**4.1. One-dimensional Dirac equation.** We first consider the equation (1.1) with one dimension. We take a bounded domain  $\Omega = (a, b)$  and assume periodic boundary conditions.

**Problem 1. Nonlinear Case.** In this example, we consider the bounded domain  $\Omega = (-32, 32)$  and the electric potential  $V(x) = \frac{x-1}{x^2+1}$ . The nonlinearity is defined as  $\mathbf{F}(\Phi) = (\Phi^* \sigma_3 \Phi) \sigma_3$  and the initial data  $\Phi_0 = (\phi_1, \phi_2)$  in (1.2) is selected as  $\phi_1(0, x) = e^{-\frac{x^2}{2}}$ ,  $\phi_2(0, x) = e^{-\frac{(x-1)^2}{2}}$ .

We first test the spatial discretization error of the proposed SEP-TS4 which is given in Figure 2. Here the reference solution is obtained by SEP-TS4 with  $\Delta t = 0.01$ ,  $N_x = 2^{11}$  and  $N_\tau = 2^8$ . The results of EEP-TS4 are similar and are omitted here. From these results, it can be observed that the

FIG. 3. Problem 1. Temporal error of NLDE (1.1) in 1D at  $t = 1$  under different  $\varepsilon$ .FIG. 4. Problem 1. Energy error (top) and mass error (bottom) of NLDE (1.1) in 1D under different  $\varepsilon$  and  $\Delta t$ .

spatial discretization in the  $x$  and  $\tau$  directions has spectral accuracy for all  $\varepsilon \in (0, 1]$ . In the following experiments, we fixed  $N_x = 2^{10}$  and  $N_\tau = 2^6$ , which is enough to achieve machine accuracy.

Subsequently, we test the temporal errors, with the exact solution obtained via the second-order Strang splitting method ([2]) using an ultra-fine time step  $10^{-6}$ . The temporal error  $err = \frac{\|\Phi^n - \Phi(t_n, \cdot)\|_{l^\infty}}{\|\Phi(t_n, \cdot)\|_{l^\infty}}$  at  $t = 1$  for varying  $\varepsilon$  are presented in Figure 3. The numerical results show that the temporal errors for both SEP-TS4 and EEP-TS4 exhibit a fourth-order convergence rate, in alignment with the theoretical bounds (3.1).

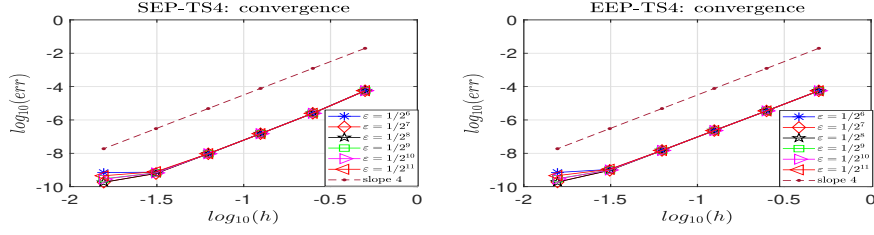
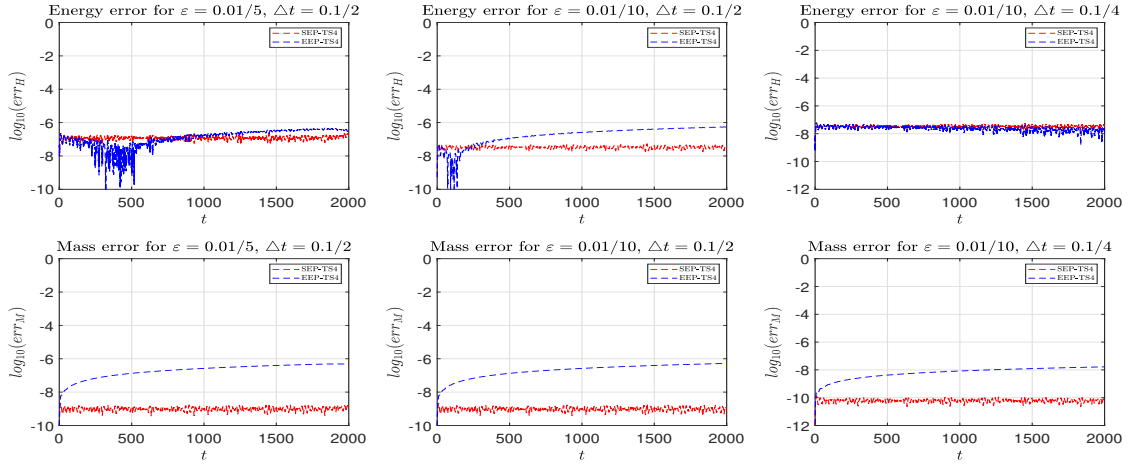
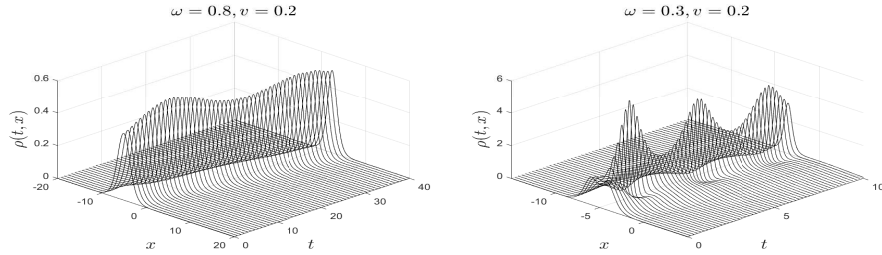
Then we study the long-term performance of the EP-TS4 integrators by investigating their numerical energy  $H(\Phi^n)$  and mass  $M(\Phi^n)$ . The conservation errors  $err_H = \frac{|H(\Phi^n) - H(\Phi^0)|}{|H(\Phi^0)|}$  and  $err_M = \frac{|M(\Phi^n) - M(\Phi^0)|}{|M(\Phi^0)|}$  are displayed in Figure 4. The result clearly illustrates that the symmetric SEP-TS4 integrator maintains perfect long-term conservation properties, whereas the non-symmetric EEP-TS4 integrator exhibits a noticeable drift in both energy and mass.

**Problem 2. Dynamics of traveling waves.** When  $\varepsilon = 1$ ,  $V(x) = 0$ ,  $\lambda_2 = 0$ , the NLDE (1.1) in 1D with  $\lambda_1 = -1$  is

$$(4.1) \quad i\partial_t \Phi = \left( -\frac{i}{\varepsilon} \sigma_1 \partial_x + \frac{1}{\varepsilon^2} \sigma_3 \right) \Phi - \Phi^* \sigma_3 \Phi \sigma_3 \Phi, \quad \mathbf{x} \in \mathbb{R},$$

which admits soliton solutions with velocity  $v$  initially placed as  $x_0$  as

$$(4.2) \quad \Phi^{ss}(x - x_0, t) = \begin{pmatrix} \sqrt{\frac{\gamma+1}{2}} & \text{sign}(v) \sqrt{\frac{\gamma-1}{2}} \\ \text{sign}(v) \sqrt{\frac{\gamma-1}{2}} & \sqrt{\frac{\gamma+1}{2}} \end{pmatrix} \Phi^{sw}(\tilde{t}, \tilde{x}).$$

FIG. 5. Problem 2. Temporal error of NLDE (4.1) in 1D at  $t = 1$  under different  $\varepsilon$ .FIG. 6. Problem 2. Energy error (top) and mass error (bottom) of NLDE (4.1) in 1D with different  $\varepsilon$  and  $\Delta t$ .FIG. 7. Problem 2. Evolution of the density  $\rho(t, x) = |\Phi(t, x)|^2$  of NLDE (4.1) initially one-humped (left) and two-humped waves (right) with  $\varepsilon = 0.01$ .

Here  $\gamma = 1/\sqrt{1-v^2}$ ,  $\tilde{x} = \gamma(x - x_0 - vt)$ ,  $\tilde{t} = \gamma(t - v(x - x_0))$ , and  $\Phi^{sw}$  is the standing wave defined as

$$(4.3) \quad \Phi^{sw}(x, t) \equiv \begin{pmatrix} \phi_1^{sw}(x, t) \\ \phi_2^{sw}(x, t) \end{pmatrix} = \begin{pmatrix} A(x) \\ iB(x) \end{pmatrix} e^{-i\omega t}, \quad 0 < \omega \leq 1,$$

where

$$A(x) = \frac{\sqrt{-\frac{2}{\lambda_1}(1-\omega^2)(1+\omega)} \cosh(\sqrt{1-\omega^2}x)}{1 + \omega \cosh(2\sqrt{1-\omega^2}x)}, \quad B(x) = \frac{\sqrt{-\frac{2}{\lambda_1}(1-\omega^2)(1-\omega)} \cosh(\sqrt{1-\omega^2}x)}{1 + \omega \cosh(2\sqrt{1-\omega^2}x)}.$$

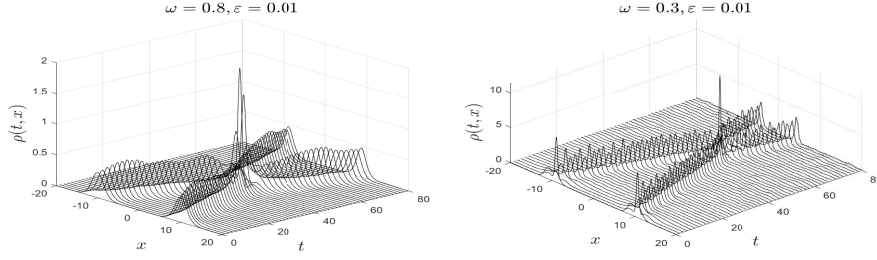


FIG. 8. *Problem 2. Evolution of the density  $\rho(t, x) = |\Phi(t, x)|^2$  of NLDE (4.1) binary collision of one-humped (left) and two-humped waves (right) with  $\varepsilon = 0.01$ .*

In this study, we adopt these soliton solutions as initial conditions to investigate the dynamics of the Dirac equation (4.1) in the nonrelativistic limit with  $\varepsilon \ll 1$ . All numerical simulations are conducted on a bounded domain  $\Omega = (-32, 32)$  with spatial mesh size  $N_x = 2^{10}$ ,  $N_\tau = 2^6$ .

It is well-established that soliton solutions exhibit two distinct profiles [51, 57]: the one-humped soliton for  $\omega \in [1/2, 1)$  and the two-humped soliton for  $\omega \in (0, 1/2)$ . Firstly, the temporal errors and long term performances of Dirac equation (4.1) are respectively given in Figures 5 and 6, where we take one-humped soliton solutions (4.2) with  $\omega = 0.8$ ,  $x_0 = -5$ ,  $v = 0.2$  as initial conditions. Fourth order uniform accuracy of the proposed integrators and long time conservations for the symmetric integrator are clearly demonstrated.

In Figure 7, we examine the evolution of a single wave in the nonrelativistic regime by selecting  $\omega = 0.8$  and  $\omega = 0.3$  with  $x_0 = -5$ ,  $v = 0.2$ . As depicted in the figure, both waves propagate to the right with oscillating amplitudes. The one-humped wave maintains its one-humped profile throughout its propagation, whereas the two-humped wave undergoes noticeable changes in its profile during its evolution.

In Figure 8, we numerically solve the NLDE (4.1) using the initial condition  $\Phi(x, 0) = \Phi_l^{ss}(x - x_l, 0) + \Phi_r^{ss}(x - x_r, 0)$ , where  $x_r = -x_l = -10$ ,  $v_l = -v_r = 0.2$ ,  $\omega_r = \omega_l = 0.8$  (0.3). These parameters describe two initial two-humped solitons with identical shapes and velocities but opposite directions [51]. In the nonrelativistic regime with  $\varepsilon = 0.01$ , two identical one-humped solitons ( $\omega = 0.8$ ) first collide and merge into a single wave, subsequently separating into two traveling waves with one-humped profiles. A similar behavior is observed for the collision of two-humped solitons.

**Problem 3. Linear Case with magnetic potential.** In this test, we demonstrate the applicability of the proposed integrators to the linear Dirac equation with magnetic potential ([5]) (4.4)

$$i\partial_t \Phi = \left( -\frac{i}{\varepsilon} \sum_{j=1}^d \sigma_j \partial_j + \frac{1}{\varepsilon^2} \sigma_3 \right) \Phi + (V(\mathbf{x}) I_2 - \sum_{j=1}^d A_j(\mathbf{x}) \sigma_j) \Phi, \quad \Phi(0, \mathbf{x}) = \Phi_0(\mathbf{x}), \quad \mathbf{x} \in \mathbb{R}^d, \quad t > 0,$$

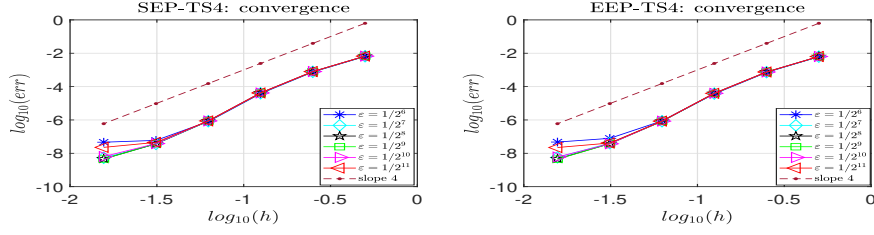
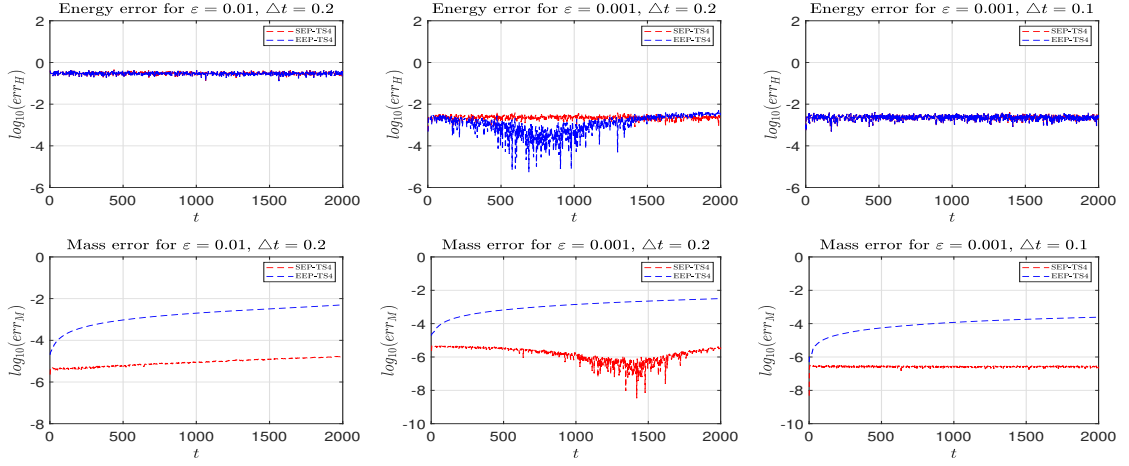
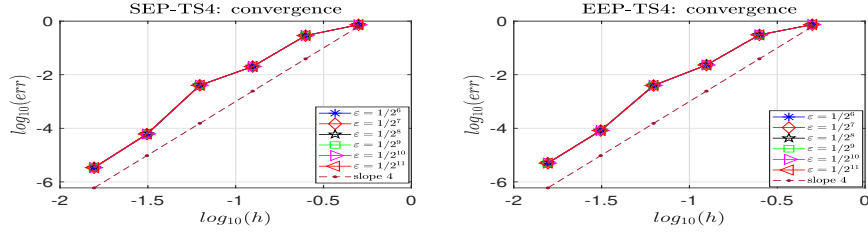
where  $I_n$  is the  $n \times n$  identity matrix for  $n \in \mathbb{N}$ ,  $V := V(\mathbf{x})$  and  $\mathbf{A} := \mathbf{A}(\mathbf{x}) = (A_1(\mathbf{x}), \dots, A_d(\mathbf{x}))^\top$  are the real-valued electrical potential and magnetic potential vector. The system (4.4) conserves the total energy

$$E(t) := \int_{\mathbb{R}^d} \left( -\frac{i}{\varepsilon} \sum_{j=1}^d \Phi^* \sigma_j \partial_j \Phi + \frac{1}{\varepsilon^2} \Phi^* \sigma_3 \Phi + V(\mathbf{x}) |\Phi|^2 - \sum_{j=1}^d A_j(\mathbf{x}) \Phi^* \sigma_j \Phi \right) d\mathbf{x} \equiv E(0), \quad t \geq 0.$$

and the total mass (1.4).

We choose  $d = 1$ , the bounded domain  $\Omega = (-32, 32)$ , the electric potential and magnetic potential as  $V(x) = \frac{1-x}{1+x^2}$ ,  $A(x) = \frac{(x+1)^2}{1+x^2}$ , and the initial data  $\Phi_0 = (\phi_1, \phi_2)$  with  $\phi_1(0, x) = e^{-\frac{x^2}{2}}$ ,  $\phi_2(0, x) = e^{-\frac{3(x-1)^2}{2}}$ . The temporal errors at  $t = 1$  under different  $\varepsilon$  are given in Figure 9 and the long time energy and mass performances are shown in Figure 10. The numerical phenomena observed are analogous to those of the first two problems.



FIG. 9. Problem 3. Temporal error of LDE (4.4) in 1D at  $t = 1$  under different  $\varepsilon$ .FIG. 10. Problem 3. Energy error (top) and mass error (bottom) of LDE (4.4) in 1D under different  $\varepsilon$  and  $\Delta t$ .FIG. 11. Problem 4. Temporal error of NLDE (1.1) in 2D at  $t = 1$  under different  $\varepsilon$ .

**4.2. Two-dimensional Dirac equation.** This subsection is devoted to the numerical experiments on the two-dimensional Dirac equation.

**Problem 4. Nonlinear case.** In the following numerical experiments, we take  $\Omega = (-16, 16)^2$ ,  $\Delta x = 1/8$ ,  $N_\tau = 2^6$ , and a honeycomb lattice potential

$$(4.5) \quad V(\mathbf{x}) = \cos\left(\frac{4\pi}{\sqrt{3}}\mathbf{e}_1 \cdot \mathbf{x}\right) + \cos\left(\frac{4\pi}{\sqrt{3}}\mathbf{e}_2 \cdot \mathbf{x}\right) + \cos\left(\frac{4\pi}{\sqrt{3}}\mathbf{e}_3 \cdot \mathbf{x}\right), \quad \mathbf{x} \in \mathbb{R}^2, \quad t \geq 0,$$

where  $\mathbf{e}_1 = (-1, 0)^\top$ ,  $\mathbf{e}_2 = (1/2, \sqrt{3}/2)^\top$ ,  $\mathbf{e}_3 = (1/2, -\sqrt{3}/2)^\top$ . Choose the initial data  $\Phi_0(\mathbf{x}) = (\phi_1(\mathbf{x}), \phi_2(\mathbf{x}))^\top$  as  $\phi_1(\mathbf{x}) = e^{-\frac{x^2+y^2}{2}}$ ,  $\phi_2(\mathbf{x}) = e^{-\frac{(x-1)^2+y^2}{2}}$ ,  $\mathbf{x} = (x, y)^\top \in \mathbb{R}^2$ .

Firstly, Figures 11 and 12 respectively display the temporal errors and long-term performance of the 2D Dirac equation (1.1). The reference solution is given by the 2D Strang splitting method with  $\Delta t = 10^{-5}$ ,  $h = 1/8$ . Fourth order uniform accuracy and long time behaviour are clearly observed.

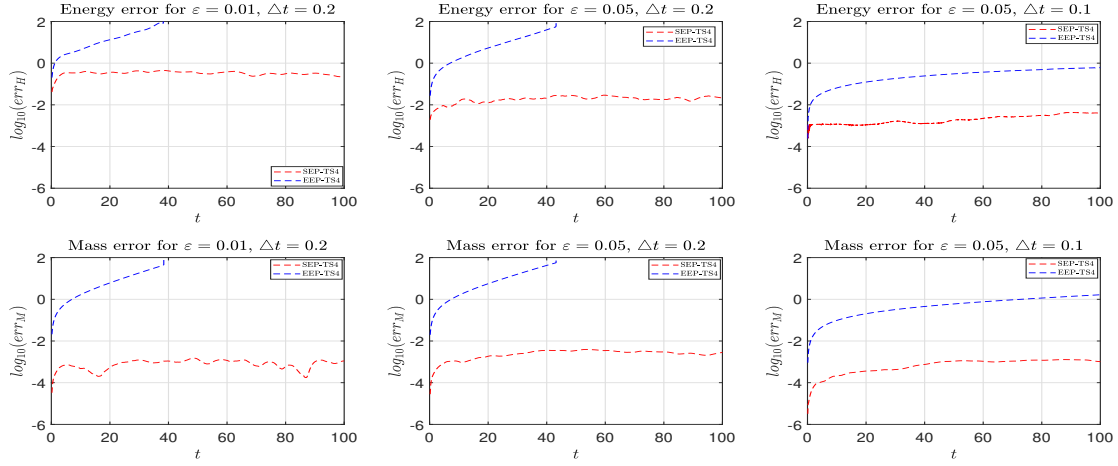


FIG. 12. Problem 4. Energy error (top) and mass error (bottom) of NLDE (1.1) in 2D under different  $\varepsilon$  and  $\Delta t$ .

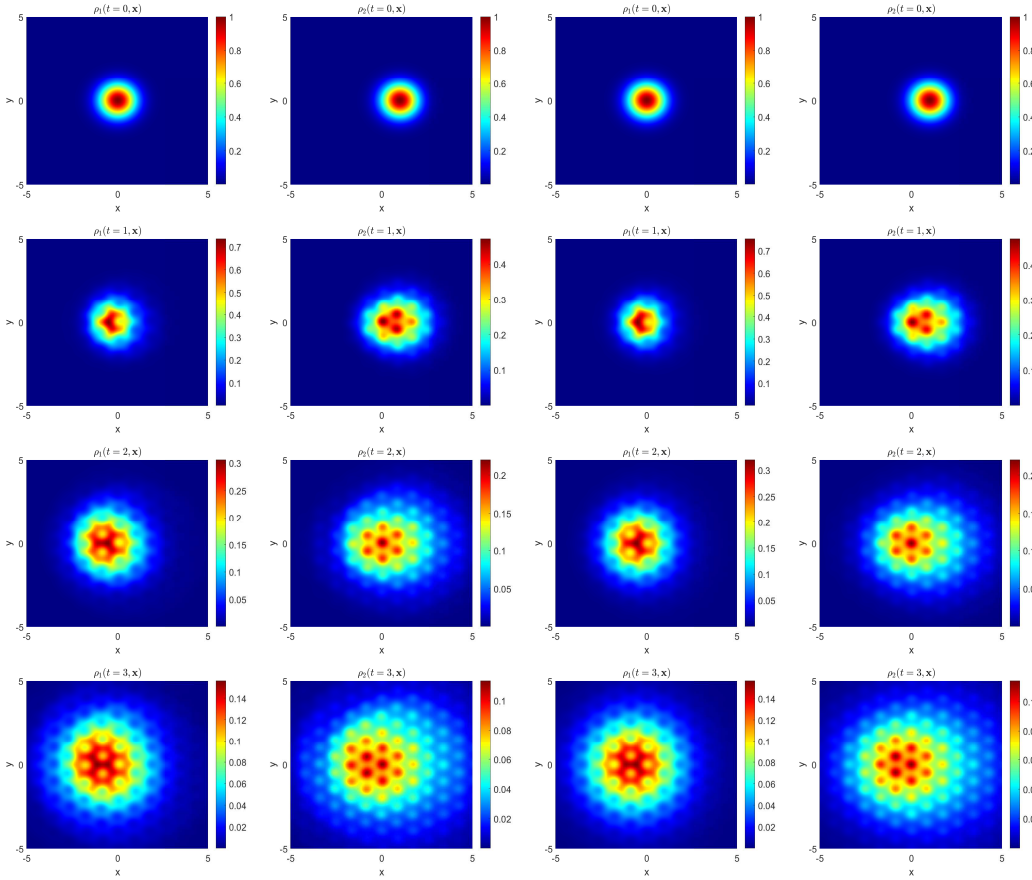


FIG. 13. Problem 4. Contour plots of the densities  $\rho_i(t, \mathbf{x}) = |\phi_i(t, \mathbf{x})|^2$ ,  $i = 1, 2$  for  $\varepsilon = 0.1$  (left two columns) and  $\varepsilon = 0.01$  (right two columns) of NLDE (1.1) in 2D under the nonlinearity  $\lambda_1 = -1$ ,  $\lambda_2 = 0$  with a honeycomb potential.

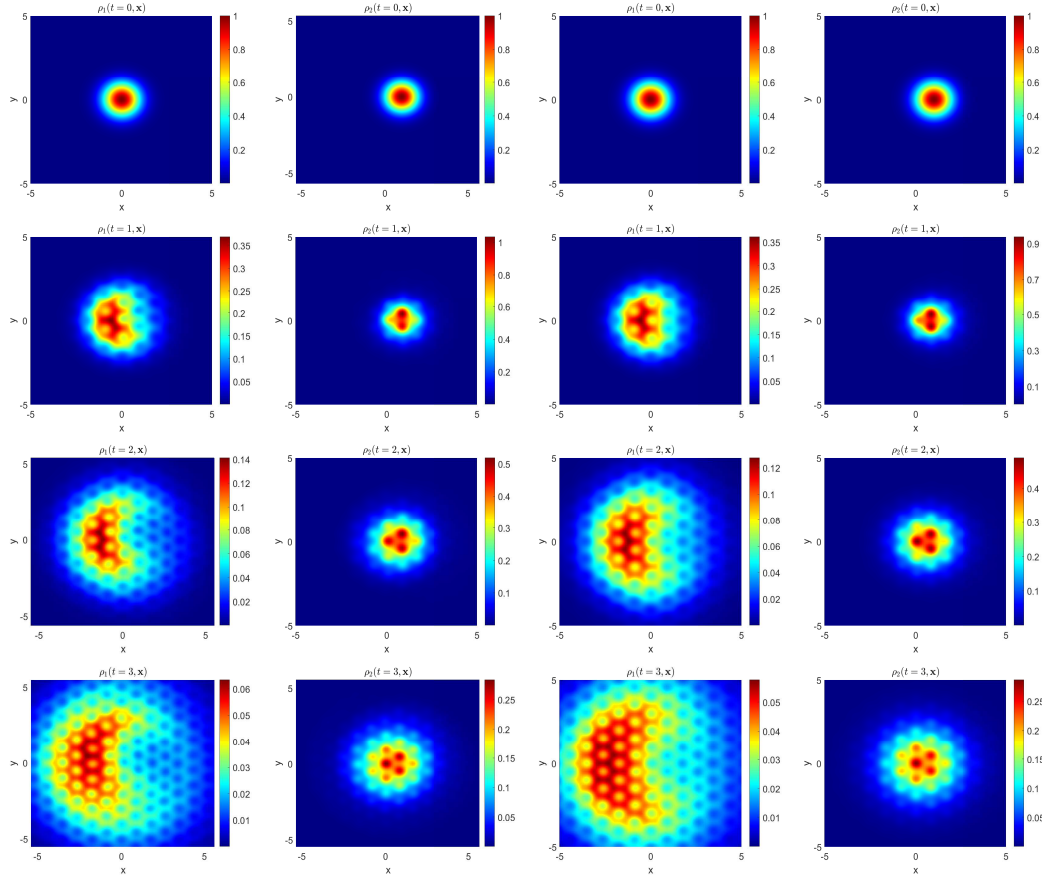
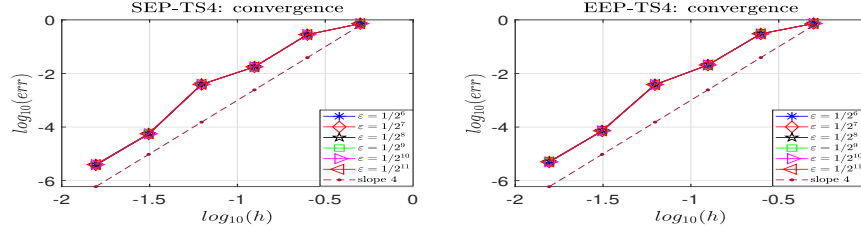
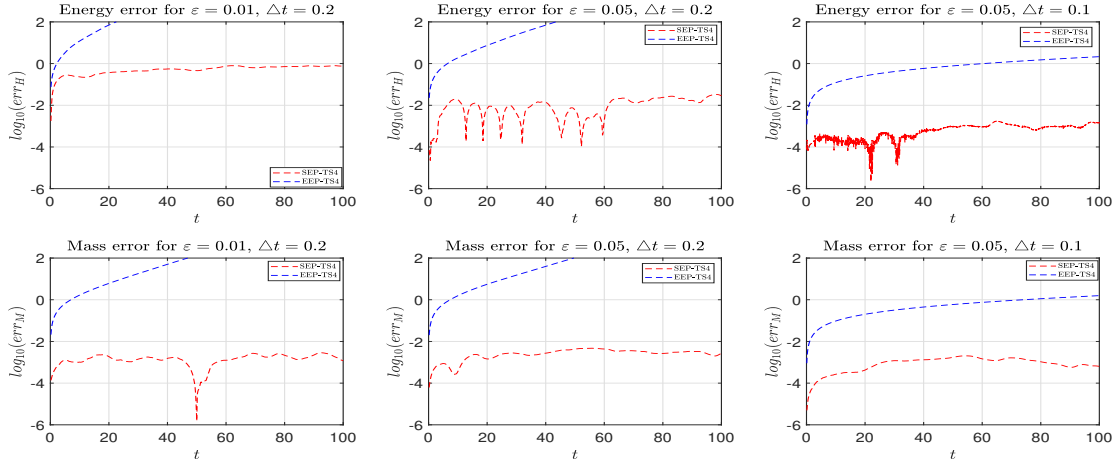


FIG. 14. *Problem 4. Contour plots of the densities  $\rho_i(t, \mathbf{x}) = |\phi_i(t, \mathbf{x})|^2$ ,  $i = 1, 2$  for  $\varepsilon = 0.1$  (left two columns) and  $\varepsilon = 0.01$  (right two columns) of NLDE (1.1) in 2D under the nonlinearity  $\lambda_1 = 0$ ,  $\lambda_2 = 1$  with a honeycomb potential.*

Then we give the dynamics of the nonlinear Dirac equation (1.1) in 2D ( $d=2$ ) by SEP-TS4 with  $\Delta t = 0.01$ . Figures 13 and 14 illustrate the densities  $\rho_j(t, \mathbf{x}) = |\phi_j(t, \mathbf{x})|^2$ ,  $j = 1, 2$ , for  $\varepsilon = 0.1$  and  $\varepsilon = 0.01$  under varying nonlinearities. As observed, for both  $\varepsilon = 0.1$  and  $\varepsilon = 0.01$ , the densities exhibit a smoother distribution across the lattice potential, and the dynamics closely resemble those of the Schrödinger-type limiting system.

**Problem 5. Linear case with magnetic potential.** As the last numerical test, we study numerically the dynamics of the linear Dirac equation (4.4) with a honeycomb lattice potential, i.e. we take  $d = 2$ ,  $A_1(\mathbf{x}) = A_2(\mathbf{x}) \equiv 0$ ,  $V(\mathbf{x})$  and initial data  $\Phi_0(\mathbf{x})$  are still taken as before. The problem is solved numerically on  $\Omega = [-10, 10]^2$  with mesh size  $\Delta x = 1/16$ ,  $N_\tau = 2^6$ . Firstly we test the time error of LDE (4.4) and the long-term performance, and the corresponding results are presented in Figures 15-16. Figure 17 depicts the densities  $\rho_j(t, \mathbf{x}) = |\phi_j(t, \mathbf{x})|^2$  ( $j = 1, 2$ ) for  $\varepsilon = 0.2$  and  $\varepsilon = 0.01$  by the SEP-TS4 schemes with time step  $\Delta t = 0.01$ . As  $\varepsilon \rightarrow 0^+$ , the relativistic effects gradually vanish, and the Dirac equation asymptotically reduces to the Schrödinger equations, leading to a smoother spatial distribution of the densities across the lattice potential.

**5. Conclusion.** In this work, we developed and analyzed two novel fourth-order integrators for solving the nonlinear Dirac equation in the nonrelativistic regime. Through a sequence of transformations of the original system, application of the two-scale formulation approach, spectral semi-discretization, and fourth-order exponential integrators, we constructed a symmetric integrator and an explicit scheme. These two integrators were rigorously proved to achieve fourth-order uniform

FIG. 15. Problem 5. Temporal error of LDE (4.4) in 2D at  $t = 1$  under different  $\varepsilon$ .FIG. 16. Problem 5. Energy error (top) and mass error (bottom) of LDE (4.4) in 2D under different  $\varepsilon$  and  $\Delta t$ .

accuracy. For the symmetric scheme, long-term energy conservation was shown by using modulated Fourier expansion. Moreover, the proposed integrators were applied to different kinds of Dirac equation. Several numerical experiments were conducted to illustrate the superior performance of the proposed integrators.

## REFERENCES

- [1] M. BALABANE, T. CAZENAVE, A. DOUADY, AND F. MERLE, Existence of excited states for a nonlinear Dirac field, Commun. Math. Phys., 119 (1988), pp. 153-176.
- [2] W. BAO, Y. CAI, AND J. YIN, Uniform error bounds of time-splitting methods for the nonlinear Dirac equation in the nonrelativistic regime without magnetic potential, SIAM J. Numer. Anal., 59 (2021) pp.1040-1066.
- [3] W. BAO, Y. CAI, X. JIA AND J. YIN, Error estimates of numerical methods for the nonlinear Dirac equation in the nonrelativistic limit regime, Sci China Math, 59 (2016), pp. 1461-1494.
- [4] W.BAO, Y.CAI, X. JIA, AND Q.TANG, A uniformly accurate multiscale time integrator pseudospectral method for the Dirac equation in the nonrelativistic limit regime, SIAM J. Numer. Anal., 54 (2016), pp. 1785-1812.
- [5] W. BAO, Y. CAI, X. JIA, AND Q. TANG, Numerical methods and comparison for the Dirac equation in the nonrelativistic limit regime, J. Sci. Comput., 71 (2017) pp. 1094-1134.
- [6] W. BAO AND Y. CAI, Mathematical theory and numerical methods for Bose-Einstein condensation, Kinet. Relat. Models, 6 (2013) pp. 1-135.
- [7] W. BAO, Y. CAI, AND X. ZHAO, A uniformly accurate multiscale time integrator pseudospectral method for the Klein-Gordon equation in the nonrelativistic limit regime, SIAM J. Numer. Anal., 52 (2014), pp. 2488-2511.
- [8] W. BAO, X. DONG, AND X. ZHAO, Uniformly accurate multiscale time integrators for highly oscillatory second order differential equations, J. Math. Study., 47 (2014), pp. 111-150.
- [9] W. BAO, Y. CAI, AND Y. FENG, Improved uniform error bounds on time-splitting methods for the long-time dynamics of the weakly nonlinear Dirac equation, IMA J. Numer. Anal., 44 (2024), pp. 654-679.
- [10] W. BAO, Y. FENG, AND J. YIN, Improved uniform error bounds on time-splitting methods for the long-time dynamics of the Dirac equation with small potentials, Multi. Model. Simul., 20 (2022), pp. 1040-1062.

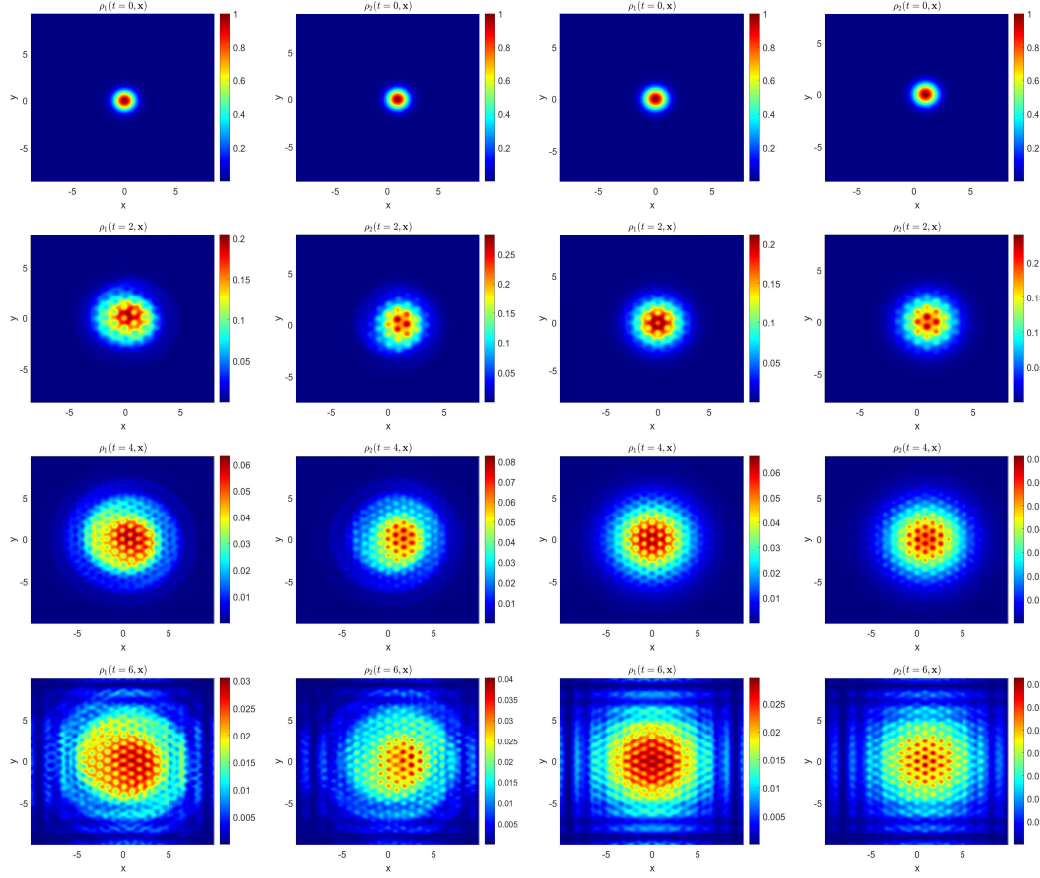


FIG. 17. Problem 5. Contour plots of the densities  $\rho_i(t, \mathbf{x}) = |\phi_i(t, \mathbf{x})|^2$ ,  $i = 1, 2$  of LDE (4.4) in 2D for  $\varepsilon = 0.2$  (left two columns) and  $\varepsilon = 0.01$  (right two columns) with a honeycomb potential.

- [11] W. BAO AND J. YIN, A fourth-order compact time-splitting Fourier pseudospectral method for the Dirac equation, Res. Math. Sci., 6 (2019).
- [12] W. BAO AND X. ZHAO, A uniformly accurate (UA) multiscale time integrator Fourier pseudospectral method for the Klein-Gordon-Schrödinger equations in the nonrelativistic limit regime, Numer. Math., 135 (2017), pp. 833-873.
- [13] W. BAO AND X. LI, An efficient and stable numerical method for the Maxwell-Dirac system, J. Comput. Phys., 199 (2004), pp. 663-687.
- [14] T. BARTSCH AND Y. DING, Solutions of nonlinear Dirac equations, J. Differential Equations, 226 (2006), pp. 210-249.
- [15] D. BRINKMAN, C. HEITZINGER, AND P. A. MARKOWICH, A convergent 2D finite-difference scheme for the Dirac-Poisson system and the simulation of graphene, J. Comput. Phys., 257 (2014), pp. 318-332.
- [16] Y. CAI AND Y. WANG, Uniformly accurate nested Picard iterative integrators for the Dirac equation in the nonrelativistic regime, SIAM J. Numer. Anal., 57 (2019), pp. 1602-1624.
- [17] Y. CAI AND Y. WANG, Uniformly accurate nested Picard iterative integrators for the nonlinear Dirac equation in the nonrelativistic regime, Multi. Model. Simul., 20 (2022), pp. 164-187.
- [18] Y. CAI AND Y. WANG, A uniformly accurate (UA) multiscale time integrator pseudospectral method for the nonlinear Dirac equation in the nonrelativistic limit regime, ESAIM Math. Model. Numer. Anal., 52 (2018), pp. 543-566.
- [19] G. CAO AND H. GAO, Mechanical properties characterization of two-dimensional materials via nanoindentation experiments, Prog. Mater. Sci. 103 (2019), pp. 558-595.
- [20] T. CAZENAVE AND L. VAZQUEZ, Existence of localized solutions for a classical nonlinear Dirac field, Commun. Math. Phys., 105 (1986), pp. 34-47.
- [21] L. CHAI, E. LORIN AND X. YANG, Frozen Gaussian approximation for the Dirac equation in semiclassical regime, SIAM J. Numer. Anal., 57 (2019), pp. 2383-2412.
- [22] S. J. CHANG, S. D. ELLIS, AND B. W. LEE, Chiral confinement: an exact solution of the massive Thirring model, Phys. Rev. D., 11 (1975), pp. 3572-3582.

- [23] PH. CHARTIER, N. CROUSEILLES, M. LEMOU, AND F. MÉHATS, Uniformly accurate numerical schemes for highly oscillatory Klein-Gordon and nonlinear Schrödinger equations, *Numer. Math.*, 129 (2015), pp. 211-250.
- [24] PH. CHARTIER, M. LEMOU, F. MÉHATS, AND X. ZHAO, Derivative-free high-order uniformly accurate schemes for highly-oscillatory systems, *IMA J. Numer. Anal.*, 42 (2022), pp. 1623-1644.
- [25] P.A.M. DIRAC, The quantum theory of the electron, *Proc. R. Soc. Lond. A*, 117 (1928), pp. 610-624.
- [26] J. DOLBEAULT, M. J. ESTEBAN, AND E. SERE, On the eigenvalues of operators with gaps: Applications to Dirac operator, *J. Funct. Anal.*, 174 (2000), pp. 208-226.
- [27] M. J. ESTEBAN AND E. SERE, Stationary states of the nonlinear Dirac equation: A variational approach, *Commun. Math. Phys.*, 171 (1995), pp. 323-350.
- [28] Y. FENG, Z. XU, AND J. YIN, Uniform error bounds of exponential wave integrator methods for the long-time dynamics of the Dirac equation with small potentials, *Appl. Numer. Math.*, 172 (2022), pp. 50-66.
- [29] F. FILLION-GOURDEAU, E. LORIN, AND A. D. BANDRAUK, Numerical solution of the time-dependent Dirac equation in coordinate space without fermion-doubling, *Comput. Phys. Commun.*, 183 (2012), pp. 1403-1415.
- [30] F. FILLION-GOURDEAU, E. LORIN, AND A. D. BANDRAUK, Resonantly enhanced pair production in a simple diatomic model, *Phys. Rev. Lett.*, 110 (2013), 013002.
- [31] R. FINKELSTEIN, R. LELEVIER, AND M. RUDERMAN, Nonlinear spinor fields, *Phys. Rev.*, 83 (1951), pp. 326-332.
- [32] J. DE FRUTOS AND J. M. SANZ-SERNA, Split-step spectral scheme for nonlinear Dirac systems, *J. Comput. Phys.*, 83 (1989), pp. 407-423.
- [33] W. I. FUSHCHICH AND W. M. SHTELEIN, On some exact solutions of the nonlinear Dirac equation, *J. Phys. A*, 16 (1983), pp. 271-277.
- [34] L.H. HADDAD AND L.D. CARR, The nonlinear Dirac equation in Bose-Einstein condensates: Foundation and symmetries, *Phys. D*, 238 (2009), pp. 1413-1421.
- [35] L. H. HADDAD, C. M. WEAVER, AND L. D. CARR, The nonlinear Dirac equation in Bose-Einstein condensates: I. Relativistic solitons in armchair nanoribbon optical lattices, *New J. Phys.*, 17 (2015), 063033.
- [36] E. HAIRER AND CH. LUBICH, Long-time energy conservation of numerical methods for oscillatory differential equations, *SIAM J. Numer. Anal.*, 38 (2000) pp. 414-441.
- [37] E. HAIRER, CH. LUBICH, AND G. WANNER, *Geometric Numerical Integration: Structure-Preserving Algorithms for Ordinary Differential Equations*, 2nd ed., Springer-Verlag, Berlin, Heidelberg, 2006.
- [38] R. HAMMER, W. POTZ, AND A. ARNOLD, A dispersion and norm preserving finite difference scheme with transparent boundary conditions for the Dirac equation in (1+1)D, *J. Comput. Phys.*, 256 (2014), pp. 728-747.
- [39] M. HOCHBRUCK AND A. OSTERMANN, Explicit exponential Runge-Kutta methods for semilinear parabolic problems, *SIAM J. Numer. Anal.*, 43 (2006), pp. 1069-1090.
- [40] M. HOCHBRUCK AND A. OSTERMANN, Exponential integrators, *Acta Numer.*, 19 (2010), pp. 209-286.
- [41] J. L. HONG AND C. LI, Multi-symplectic Runge-Kutta methods for nonlinear Dirac equations, *J. Comput. Phys.*, 211 (2006), pp. 448-472.
- [42] Z. HUANG, S. JIN, P. A. MARKOWICH, C. SPARBER, AND C. ZHENG, A time-splitting spectral scheme for the Maxwell-Dirac system, *J. Comput. Phys.*, 208 (2005), pp. 761-789.
- [43] M. LEMOU, F. MÉHATS AND X. ZHAO, Uniformly accurate numerical schemes for the nonlinear Dirac equation in the nonrelativistic limit regime, *Commun. Math. Sci.*, 15 (2017), pp. 1107-1128.
- [44] J. LI, Energy-preserving exponential integrator Fourier pseudo-spectral schemes for the nonlinear Dirac equation, *Appl. Numer. Math.*, 172 (2022), pp. 1-26.
- [45] J. LI, Explicit and structure-preserving exponential wave integrator Fourier pseudo-spectral methods for the Dirac equation in the simultaneously massless and nonrelativistic regime, *Calcolo*, 61 (2024).
- [46] K. LIU, B. WANG, AND X. ZHAO, Solving long-time nonlinear Schrödinger equation by a class of oscillation-relaxation integrators, *SIAM Multi. Model. Simul.*, 23 (2025), pp. 313-338.
- [47] P. MATHIEU, Soliton solutions for Dirac equations with homogeneous nonlinearity in (1+1) dimensions, *J. Phys. A*, 18 (1985), pp. L1061-L1066.
- [48] K. S. NOVOSELOV, A. K. GEIM, S. V. MOROZOV, D. JIANG, M. I. KATSNELSON, I. V. GRIGORIEVA, S. V. DUBONOS, AND A. A. FIRSOV, Two-dimensional gas of massless Dirac fermions in graphene, *Nature*, 438 (2005), pp. 197-200.
- [49] J. W. NRAUN, Q. SU, AND R. GROBE, Numerical approach to solve the time-dependent Dirac equation, *Phys. Rev. A*, 59 (1999), pp. 604-612.
- [50] F. SCHEDIN, A. GEIM, S. MOROZOV, E. HILL, P. BLAKE, M. KATSNELSON, AND K. NOVOSELOV, Detection of individual gas molecules absorbed on graphene, *Nat. Mater.*, 6 (2007), pp. 652-655.
- [51] S. SHAO AND H. TANG, Interaction for the solitary waves of a nonlinear Dirac model, *Phys. Lett. A*, 345 (2005), pp. 119-128.
- [52] J. SHEN, T. TANG, AND L. WANG, *Spectral Methods: Algorithms, Analysis and Applications*, Springer, 2011.
- [53] K. TAKAHASHI, Soliton solutions of nonlinear Dirac equations, *J. Math. Phys.*, 20 (1979), pp. 1232-1238.
- [54] B. WANG AND X. ZHAO, Geometric two-scale integrators for highly oscillatory system: uniform accuracy and near conservations, *SIAM J. Numer. Anal.*, 61 (2023), pp. 1246-1277.
- [55] Y. WANG AND X. ZHAO, Symmetric high order Gautschi-type exponential wave integrators pseudospectral method for the nonlinear Klein-Gordon equation in the nonrelativistic limit regime, *J. Numer. Anal. Model.*, 15 (2018), pp. 405-427.
- [56] H. WU, Z. HUANG, S. JIN, AND D. YIN, Gaussian beam methods for the Dirac equation in the semi-classical regime, *Comm. Math. Sci.*, 10 (2012), pp. 1301-1315.
- [57] J. XU, S. SHAO, AND H. TANG, Numerical methods for nonlinear Dirac equation, *J. Comput. Phys.*, 245 (2013), pp. 131-149.